AD-A091 816 REGIS COLL RESEARCH CENTER WESTON MA F/G 4/1
SPACE ENVIRONMENTAL STUDIES: INSTRUMENTATION AND DATA ANALYSIS --ETC(U)
SEP 80 F RICH, P B ANDERSON F19628-77-C-0122
UNCLASSIFIED AFGL-TR-80-0218 NL

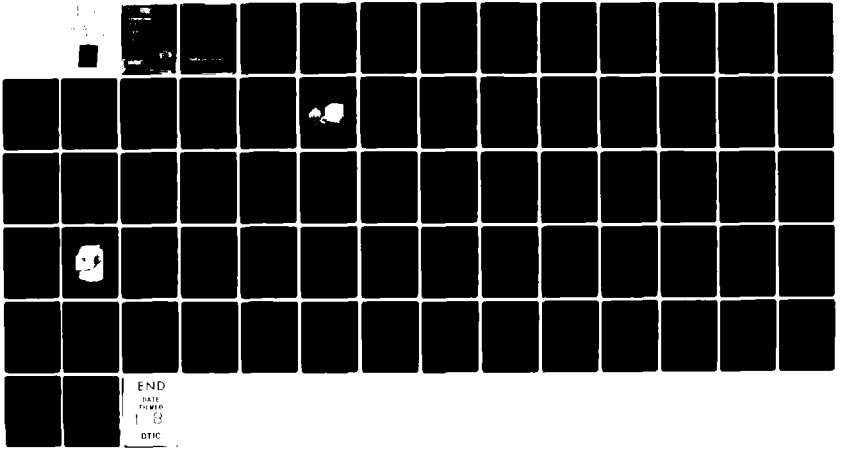

END
DATE FILMED
1 8
DTIC

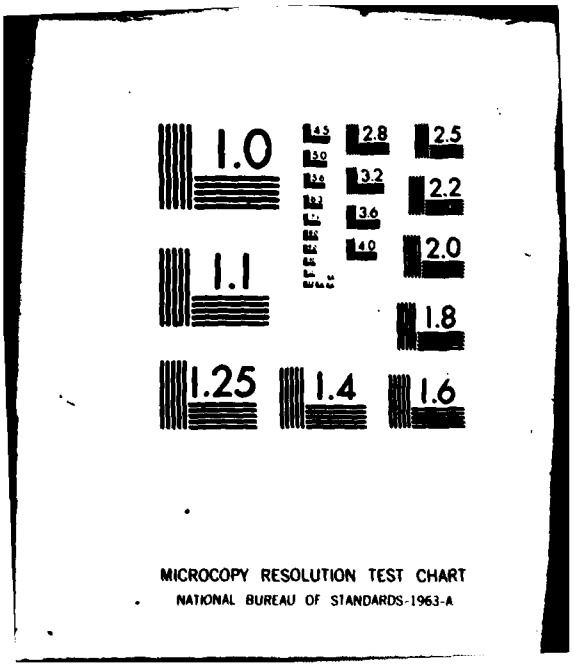
1.0
1.1
1.25
1.4
1.6
1.8
2.0
2.2
2.5
2.8
3.2
3.6
4.0
4.5
5.0
5.6
6.3
MICROCOPY RESOLUTION TEST CHART
NATIONAL BUREAU OF STANDARDS-1963-A

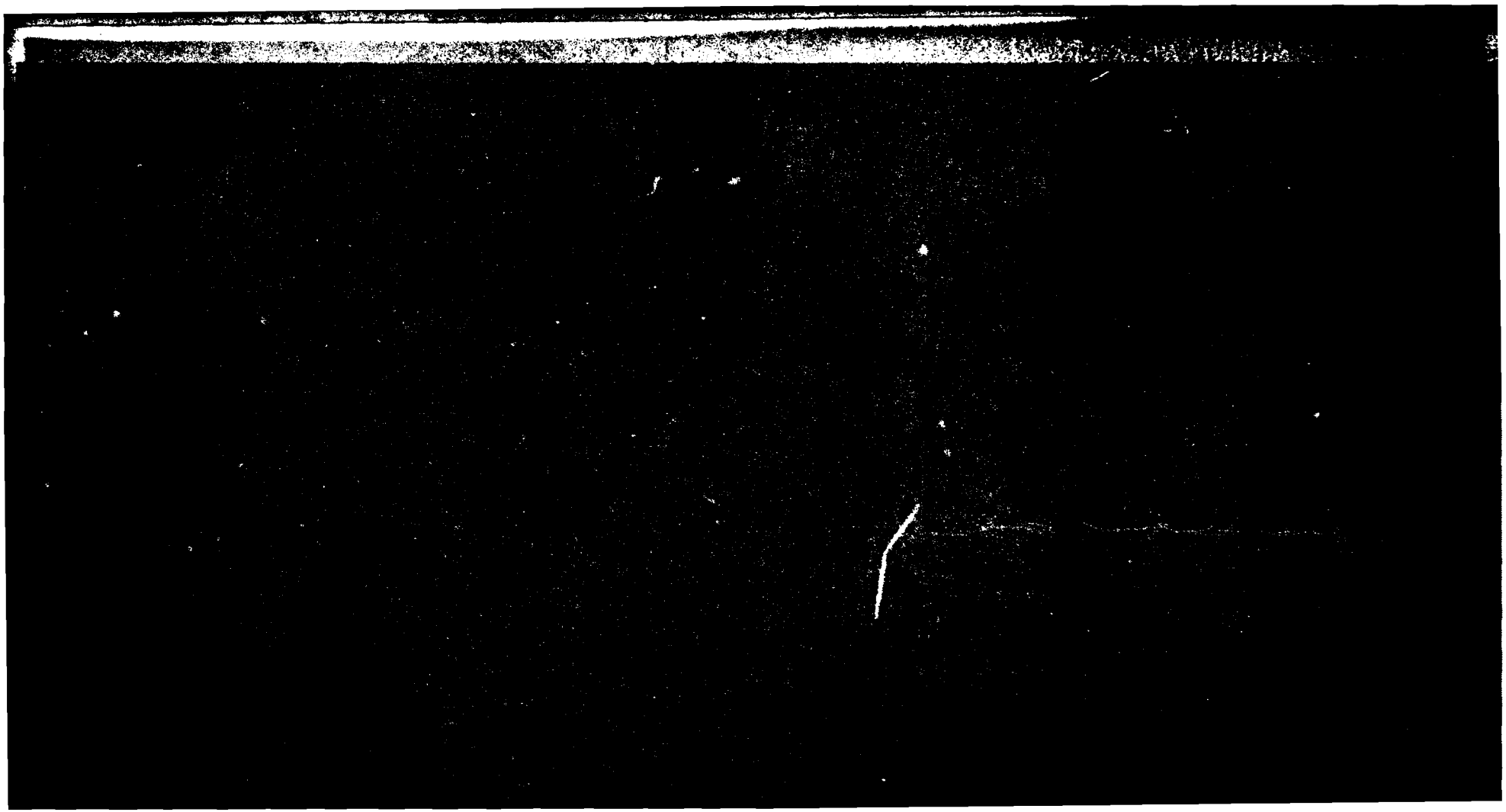

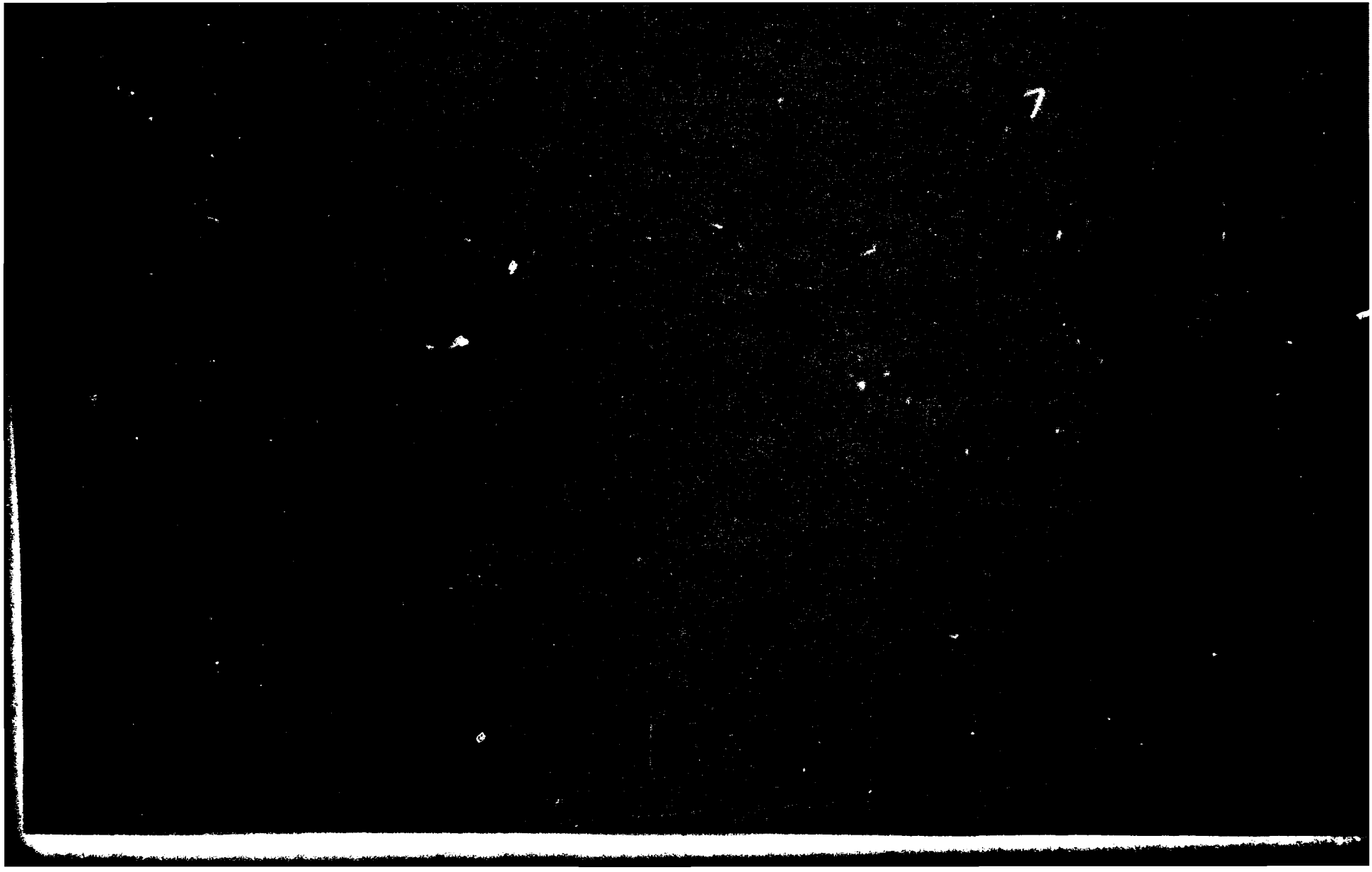

unclassified

SECURITY CLASSIFICATION OF THIS PAGE (When Data Entered)

REPORT DOCUMENTATION PAGE	READ INSTRUCTIONS BEFORE COMPLETING FORM
1. REPORT NUMBER: AFGL-TR-80-0218	2. GOVT ACCESSION NO.: AD-A091 816
	3. RECIPIENT'S CATALOG NUMBER
4. TITLE (and Subtitle): SPACE ENVIRONMENTAL STUDIES: INSTRUMENTATION AND DATA ANALYSIS RELATED TO THE IONOSPHERE.	5. TYPE OF REPORT & PERIOD COVERED: FINAL REPORT 15 MAY 77 — 31 MAY 80
	6. PERFORMING ORG. REPORT NUMBER
7. AUTHOR(s): FREDERICK J. RICH, PETER B. ANDERSON	8. CONTRACT OR GRANT NUMBER(s): F19628-77-C-0122
9. PERFORMING ORGANIZATION NAME AND ADDRESS: Regis College Research Center, 235 Wellesley St., Weston, Ma 02193	10. PROGRAM ELEMENT, PROJECT, TASK AREA & WORK UNIT NUMBERS: 61102F, 2311G2AE, 17 1G2
11. CONTROLLING OFFICE NAME AND ADDRESS: Air Force Geophysics Laboratory, Hanscom AFB, MA 01731, Contract Monitor/S.C. Bredesen, PHG	12. REPORT DATE: 2 Sept 1980
	13. NUMBER OF PAGES
14. MONITORING AGENCY NAME & ADDRESS(if different from Controlling Office)	15. SECURITY CLASS. (of this report): UNCLASSIFIED
	15a. DECLASSIFICATION/DOWNGRADING SCHEDULE

16. DISTRIBUTION STATEMENT (of this Report)

APPROVED FOR PUBLIC RELEASE: DISTRIBUTION UNLIMITED

17. DISTRIBUTION STATEMENT (of the abstract entered in Block 20, if different from Report)

18. SUPPLEMENTARY NOTES

19. KEY WORDS (Continue on reverse side if necessary and identify by block number)

ionosphere
thermal plasma
Defense Meteorological Satellite Program
Special Sensor, Ions and Electrons (SSIE)
Special Sensor, Ions, Electrons, Scintillation (SSIES)
S3-2
S3-3
SCATHA
Auroral ionosphere
Magnetosphere
Magnetic fields

20. ABSTRACT (Continue on reverse side if necessary and identify by block number)

The objective of this contract has been to design instrumentation for the Plasma, Particles and Field Branch, Space Physics Division of the Air Force Geophysics Laboratory and to analyze data from these instruments and related instruments flown on the same vehicles. In particular, the design and check out of the thermal plasma instruments for SCATHA (SC5) and for DMSP Flights 2, 4 and 5 of the Block 5D series has been done. Design work for DMSP Flights 6 through 10 has also been done. The data analysis has been done to understand and improve the quality of future instruments. For example, the electronics for the thermal plasma exper

DD FORM 1 JAN 73 1473 EDITION OF 1 NOV 65 IS OBSOLETE

unclassified

409411

lments on Flights 4 through 7 was done after an unexpected vehicle electrostatic potential problem was identified from the Flight 2 in-flight data records. The data analysis was also done to improve the general knowledge of the ionosphere.

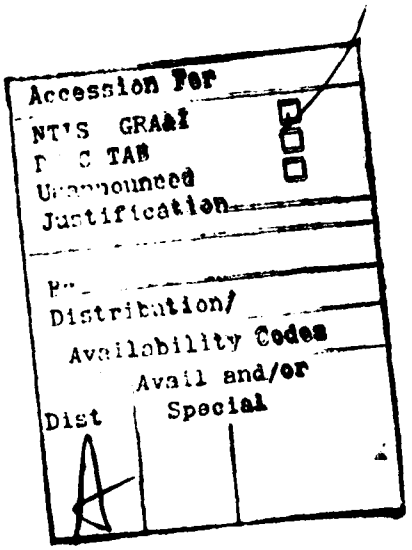

SPACE ENVIRONMENTAL STUDIES:

INSTRUMENTATION AND DATA ANALYSIS RELATED

TO THE IONOSPHERE

I. INTRODUCTION

The stated objectives of the work undertaken for contract F19628-77-C-0122 between Regis College and the Air Force Geophysics Laboratory were:

a. Design and develop instruments for a DMSP follow-on mass spectrometer experiment.

b. Design and develop instrumentation for the measurement of the electrical environment of the Spacelab and Space Shuttle Orbiter.

c. Design and develop low energy plasma instrumentation for satellites to be launched from the Space Shuttle Orbiter.

d. Design and develop instrumentation for materials investigation using the long-duration exposure facility to be lauched from the Space Shuttle Orbiter.

e. Analyze and interpret flight data from the Air Force S3-2 satellite (1) to isolate the relative contributions of soft particle precipitation and bulk plasma motion in determining ionospheric and magnetospheric current systems, (2) to determine the convective flow in the ionosphere and magnetosphere using the vector electric field measurements, (3) to ascertain the regions where and under what conditions anomalous resistivity exists in the ionosphere.

f. Analyze and interpret flight data from the Air Force S3-3 satellite to investigate the convective electric fields over the altitude range 280-8000 km using the plasma motion monitor measurements and to investigate satellite sheath and wake effects.

g. Analyze and interpret flight data from the DMSP satellite (1) to study plasma scale heights, (2) to study the ion and electron temperature profiles, (3) to study electron irregularities and gradients in the ionosphere, (4) to investigate the critical frequency in the F region.

h. Analyze and interpret flight data from the SCATHA satellites (1) to study the variations in the satellite potential, (2) to investigate the low energy ion and electron flux and energy spectra, (3) to study the plasma flow at synchronous altitudes, (4) to assess the effectiveness of ion and electron guns for satellite potential control.

Objective (a) has been carried out in full during this contract although not exactly in the manner originally anticipated. The follow-on instrument to the original thermal plasma sensor on DMSP has become the SSIES (Special Sensor, Ion, Electrons and Scintillation). As a follow-on instrument was being considered, the weight and power requirements of a mass spectrometer versus the needs of the Air Force caused the mass spectrometer to be dropped. Instead, the electronics for the thermal ion and electron sensor have been greatly improved and a passive ion trap capable of measuring fluctuations in the plasma up to 12 KHz has been added. The expected result is a more accurate and finer spatial resolution of the ion and electron temperature and density and a determination of the small scale density irregularities which are capable of causing phase and amplitude scintillations of radio signals passing through the ionosphere. For example, the highest plasma irregularity frequency to be observed is in the range 5.6 to 12 KHz which corresponds to a irregularity scale size of approximately one meter. In addition to the development of SSIES, objective (a) has been met through the addition of bias potentials between the SSIE instruments and the DMSP satellite for flights

4 through 7. This addition became necessary when the analysis of the early data from the flight 2 SSIE showed that the vehicle potential can get to -30V in sunlight due to the design of the solar panels. The SSIE had been designed with an expected vehicle potential of -3V to +1V which is typical for satellites in low altitude orbits.

Objectives (b) through (d) have required a very low level of effort due to the failure of the Air Force Geophysics Laboratory to get approval for early rides on the Shuttle and due to the extensive schedule slippage of the Shuttle. Work under these objectives was confined to providing input for the proposals for rides on the Shuttle.

Objective (e) has been extensively pursued under this contract, a large number of scientific reports and papers, which are described later, have resulted from the analysis of the S3-2 data. The quality of the S3-2 data has been very good and the quantity of S3-2 data is extensive. Because the physics of the ionosphere is a very complex topic, it is expected that much more work with the S3-2 data remains to be done using the work done under this contract as a building block.

Objective (f) has been pursued through analysis of the thermal electron data from the S3-3 Langmuir probe. It has been found that the temperature gradient at mid-latitudes is significantly less above 3000 km than it is near 1000 km altitude.

Objective (g) has been pursued to the extent of several studies related to the plasma density variations near the equator near equinox and to plasma characteristics directly related to the functioning of the hardware. Some

software development has also been done to improve the quality of future data analysis. Because the flight 2 instrument provided two and a half years of nearly continuous data and the flight 4 instrument provided seven months of nearly continuous data, there remains a great wealth of data that can be usefully investigated in the future.

Objective (h) consisted only of preparing the thermal plasma instrument (SC5) for the SCATHA launch and beginning the in-flight check out. Unfortunately the instrument failed after a few minutes of operation in space for unexplained reasons. Thus there has been no data available for scientific analysis.

The remainder of this report consists of describing in brief the work accomplished under this contract. The next section describes the engineering development work. The following section describes the scientific data analysis work. At the end of this report there is a bibliography of publications generated as a result of work done under this contract. For details about projects mentioned in this report, the reader is referred to that bibliography.

During the course of this contract, engineering services have been provided by Peter Anderson, Donald Girouard and Robert Shupe. Scientific data analysis services have been provided by Drs. Frederick Rich, Wm. Burke, Muhktar Ahmed, Michael Kelley, Mary Anne Doyle, Balram Prasad and Eugene Young.

II.

DESIGN AND DEVELOPMENT OF ELECTRICAL AND MECHANICAL INSTRUMENTS FOR SCIENTIFIC EXPERIMENTS

PETER B. ANDERSON

1. INTRODUCTION

This section describes the engineering activities carried out during the contract period. Individual areas are subdivided for clarity.

2. SCATHA SATELLITE (SC6-1, -2, and -3)

The Thermal Plasma Analyzer was designed under a previous Regis College contract, F19628-75-C-0081. The development of this instrument has continued under the present contract. As described in Technical Report AFGL-TR-77-0119, SC6 was designed to measure the direction and magnitude of the plasma bulk motion, the density and temperature of the plasma 'bath' in which the satellite is immersed, and investigate spacecraft-plasma interaction mechanisms by measuring fluctuation in vehicle potential and charging and discharge currents to the satellite due to environmental factors such as solar illumination, satellite motion, plasma temperature, density, and motion variations during quiet and disturbed conditions. It was also aimed at studies of these properties under controlled conditions when the spacecraft potential is varied by means of an electron gun.

The Thermal Plasma Analyzer consisted of three gridded sensors and an electronics package (SC6-3). Two sensors (SC6-1) were mounted on a boom 3 meters from the nearest space vehicle body mounted components. The third sensor (SC6-2) was body-mounted on the conducting end of the space vehicle. The normal to the aperture of one boom sensor is parallel to the normal to the aperture of the surface sensor and also parallel to the space vehicle spin momentum vector. The second boom sensor normal is perpendicular to the spin vector. The experiment was designed to measure, by retarding potential analy-

sis, the environmental electron and ion densities in the range 10^{-1} to 10^{4} per cm^3 and particle energies in the range 0.1 to 100 eV.

Basic mechanical design for the gridded probes is shown in Figure 2-1. The combined measurements from the surface mounted sensor and the boom mounted

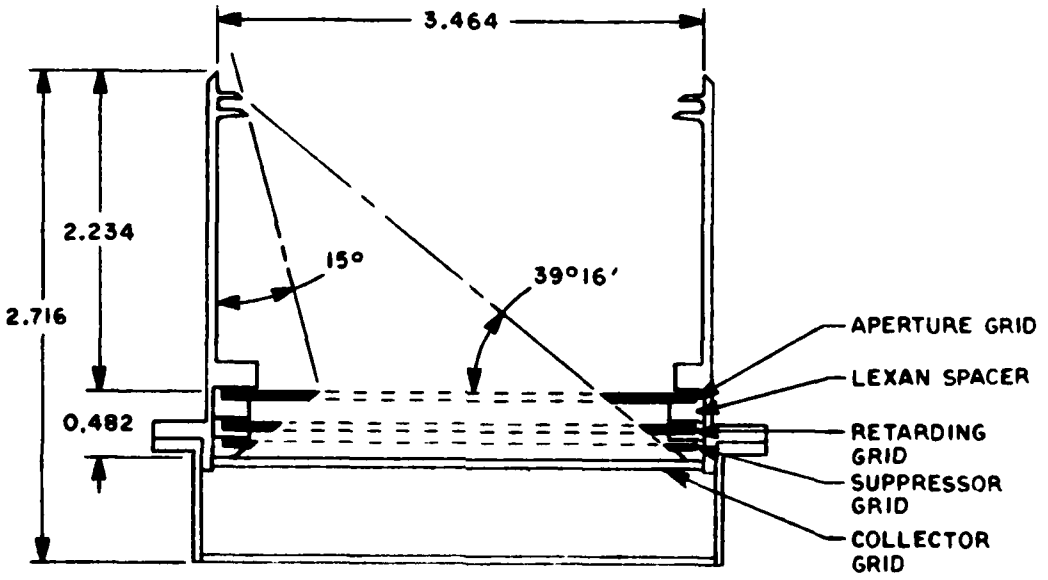

Figure 2-1: SCATHA surface and boom mounted instruments.

units made it possible to ascertain the influence of photoelectrons from the spacecraft surface. Photoelectron production within the sensor was further minimized by restricting the sensor aperture field of view to a 15^{o} half-angle cone. Depending on the voltage of the collector and stepped (retarding) grid, electrons or positive ions were measured. During disturbed conditions the vehicle potential can exceed 100V negative. In this case, the potential was determined from the positive ion sensor where the thermal ions arrived at the vehicle with average energies equal to their thermal energy plus that imparted by the energy equivalent of the spacecraft potential.

The electrical configuration of the sensor is shown in Figure 2-2. Using ground commands A, B, and C, the boom and surface mounted sensors were operated in a large number of ion or electron modes. Commands D, E, F, and G select eight (8) aperture-bias levels ranging from -50V to +50V.

The system block diagram (Figure 2-3) shows the major experiment components in addition to specific circuits designed and developed for the main electronics package SC6-3. Each sensor's electrometers were independently commandable to measure either ions or electrons and were automatic linear range-switching current to voltage amplifiers. To achieve the various operation modes of the experiment, several fixed and varying voltage signals must be periodically applied to the electrometer common and sensor elements. To do this, the electrometer common was electrically floating with respect to the system common or spacecraft ground. Since each electrometer output voltage was consequently "riding on" the varying signals being applied to the electrometer common, level shifter circuits were employed to reference the 0-5V output signal to system common. Each level shifter circuit is a differential operational amplifier which measured the difference between the electrometer common and the electrometer output. Timing and control circuitry was designed to time the system program which was clocked from a spacecraft-provided $1\,H_z$ pulse.

Two sweep (step generators) circuits were used for stepping the sensor grid elements and the electrometer floating common. The power converter section contained all of the secondary voltage circuits and the commandable bias supply. The circuitry for the step generators, bias supply and power converter was developed under a separate contract.

After a successful satellite launch on 30 Jan 79, SC6 experienced a par-

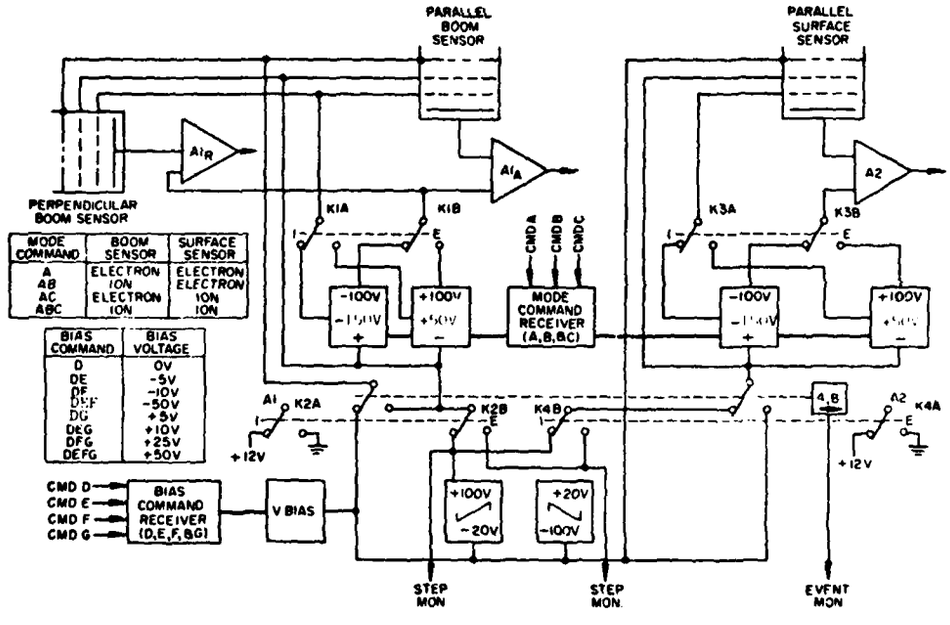

MODE COMMAND	BOOM SENSOR	SURFACE SENSOR
A	ELECTRON	ELECTRON
AB	ION	ELECTRON
AC	ELECTRON	ION
ABC	ION	ION

BIAS COMMAND	BIAS VOLTAGE
D	0V
DE	-5V
DF	-10V
DEF	-50V
DG	+5V
DEG	+10V
DFG	+25V
DEFG	+50V

Figure 2-2: SCATHA Sensor Electrical Configuration

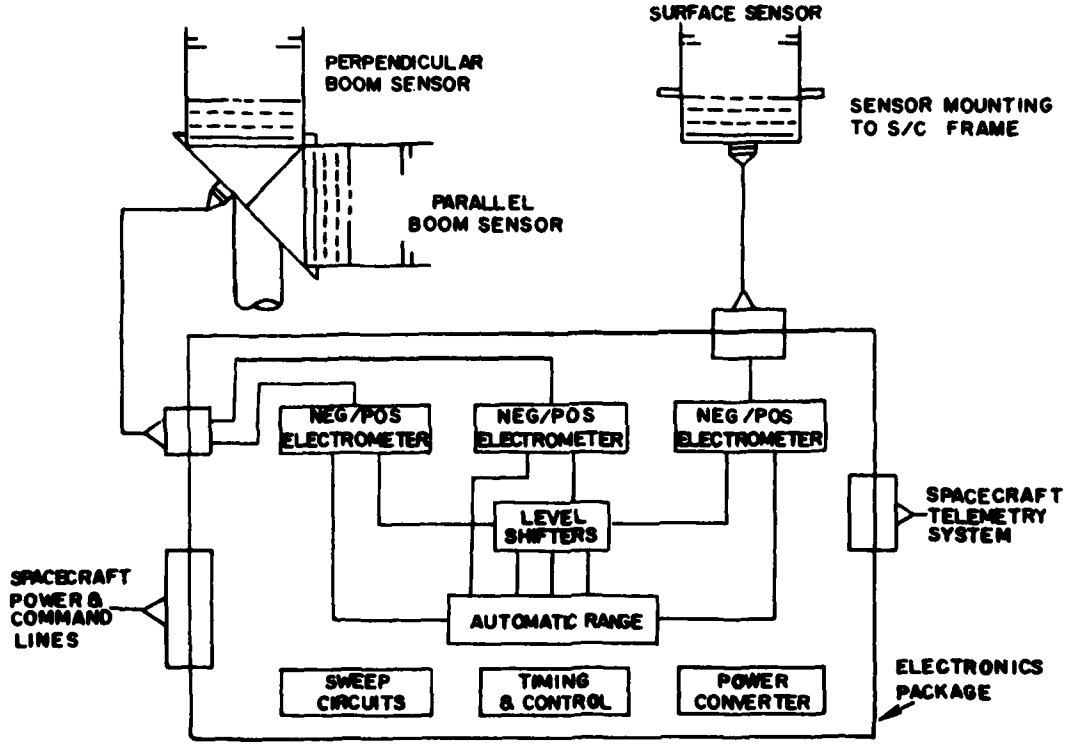

Figure 2-3: SCATHA System Block Diagram

tial failure during the initial checkout on 9 FEB 79. During the initial checkouts, the experiment (SC6) operated faultlessly for approximately 8 minutes after which a transient type response was noticed on the electrometer outputs. A few seconds later, all of the telemetry outputs were observed to decrease to about 30% below normal. However, even with this anomaly the system was still functioning in all respects.

Post analysis has been inconclusive as to the exact cause of the failure and as to which component might have failed. It is known that the electrometer output from SC6-2 sensor has an offset voltage which keeps I-2 in saturation, that the DC to DC power converter is operating in the current limit mode, and that all secondary voltages dropped gradually by 30% after being on for several seconds.

AFGL has a backup SC6-3 Electronics Package which was used as a diagnostic aid. The diagnosis was centered around the circuits in the experiment and the associated sensors. Satellite data has indicated that the spacecraft potential was normal which down plays any theory of a high potential discharge on either one of the sensors. Therefore, attention was focused on any one sensor element shorting to another and circuit components across the secondary voltage lines from the DC to DC power converter. Shorting connections to the sensor elements in the backup SC6-3 Electronics Package did not reproduce the same flight symptons. Loading the secondary voltage lines did drive the power converter into current limit mode instantly. However, it is inconceivable to have a single component, as used in the design, reproduce all of the symptoms in flight.

The contractor for the DC to DC power converter design investigated pos-

sible failure modes in their section, however, their findings were inconclusive. They did conclude that anyone of several components could have caused the failure.

EMI testing was also done on the back up SC6-3 Electronics Package. Transients were injected onto the power buss and when the transient levels were increased beyond the maximum specified, the DC to DC power converter's input circuitry was damaged. In this failure mode, the converter did not draw any current which is not what was experienced in flight (current limit mode).

Thirteen trips were made in support of the SC6 experiment. Seven trips were made to Martin-Marietta, Denver, for EMC meetings, bench tests, all modes testing, thermo-vacuum tests, and integrated system test (IST). Three trips were made to Cape Canaveral Air Force Station in support of prelaunch and launch activities. Also, 3 trips were made to Sunnyvale Satellite Control Facility in support of prelaunch and post launch activities.

3. DMSP SATELLITE SERIES (SSI/E and SSIES)

(a) The objective of the Ionosphere Plasma Monitor (SSI/E) is to obtain critical information from the DMSP Block 5D Satellite Series about the characteristics of the plasma above the peak of the F region which is required by the Air Force for HF and UHF communication systems. Development of the SSI/E instrument was completed under Regis College contract F19628-75-C-0081 and is described in Technical Report AFGL-TR-77-0119. It was designed to make in-situ measurements of topside plasma scale height, small scale ionization irregularities and F-region critical frequencies. Measurements are achieved by means of boom-

mounted electrostatic sensors which are electrically connected to an electronic package as shown in Figure 2-4. One sensor (planar electrostatic analyzer) measures environmental ion temperature and average ion mass, the second (spherical electrostatic analyzer) measures thermal electron density, temperature and satellite potential along the satellite orbit.

The first SSI/E instrument (S/N 1) was successfully launched on the DMSP F2 Satellite. However, examination of initial SSI/E data from the F2 spacecraft has shown the following: 1. The instrument was functioning properly. 2. The satellite vehicle potential is highly variable in the negative direction. It was between -6 and <-20 volts with respect to the plasma over about ½ of each orbit. On the remainder of the orbit it varied from +0.5 to -6 volts. Accurate data for the F2 instrument design requires that the spacecraft vehicle potential does not go more than 5 volts negative. This negative potential on the DMSP satellite is due to exposed positive conductors on the solar array panel and inadequate spacecraft conductive area at satellite ground.

To correct the above problem, several circuit design changes were made to the SSI/E Instruments for flights F4 thru F7. The revised system bias block diagram (Figure 2-5) shows the major experiment components with specific circuits outlined within the Electronics Package. In order to offset the negative vehicle potential, an auxiliary bias supply was added to the bottom of the Electronics Package. With an additional level command circuit, the bias supply can now be commanded to levels of 0.0V, +6.5V, +16V, or +26V as shown in Table 2-1. In addition, the ion and electron sweep circuits were redesigned to electrically "float" on the commanded bias output level. To accommodate these changes, new printed circuit board designs were completed for the Level

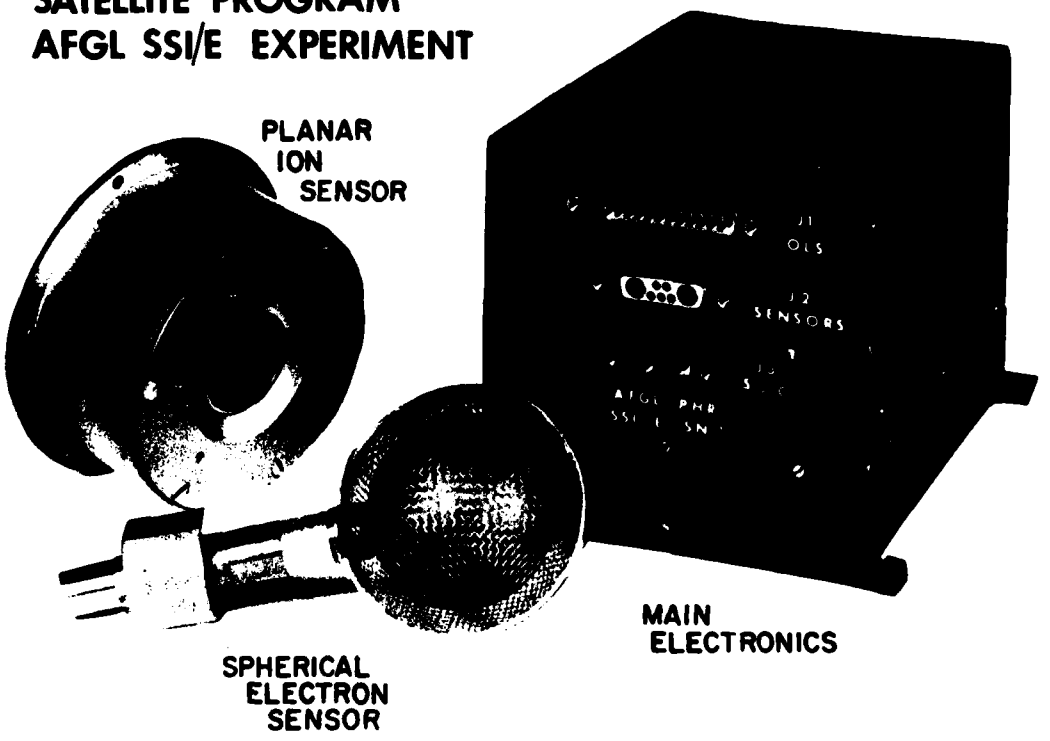

Figure 2-4: DMSP SSI/E Flight Components

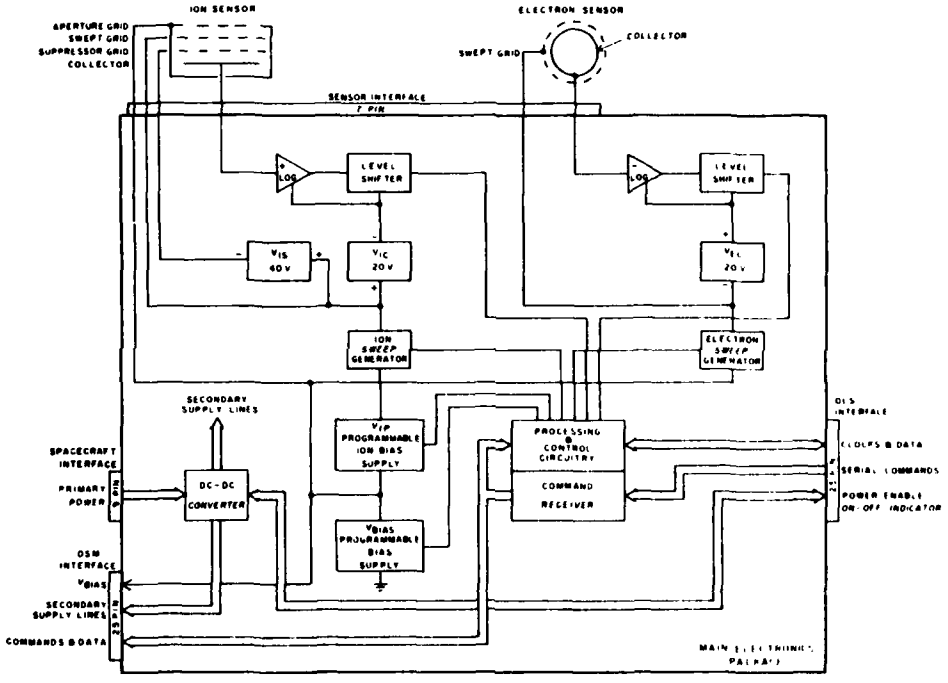

Figure 2-5: SSIES System Block Diagram

TABLE 2-1

DMSP BIAS MODE LEVEL COMMANDS

F2

MODE	SSIEMDE MODE SELECTION	SSIESPL SPARE 1 SELECTION	BIAS	MODE MON.
1	0V (ON)	N.A.	1.50V	3.50V
*2	5V (OFF)	N.A.	0.00V	1.50V

F4, F5

MODE	SSIEMDE MODE SELECTION	SSIESPL SPARE 1 SELECTION	BIAS	MODE MON.
1	0V (ON)	0V (OFF)	0V	0.00V
*2	5V (OFF)	0V (OFF)	6.5V	1.00V
3	0V (ON)	5V (ON)	16V	2.46V
4	5V (OFF)	5V (ON)	26V	4.00V

F6, F7

MODE	SSIEMDE MODE 1 SELECT	SSIESPL MODE 2 SELECT	BIAS	MODE MON.
1	0V (ON)	0V (ON)	0V	0.00V
2	5V (OFF)	0V (ON)	6.5V	1.00V
3	0V (ON)	5V (OFF)	16V	2.46V
*4	5V	V (OFF)	26V	4.00V

* Initial OLS Power On Conditions

Shifter, Sweep, Timer, and Auxiliary Bias Supply boards. Other design changes include the Log electrometer sensitivities and Digital Data Interface (DDI) output circuitry. The DMSP telemetry system (OLS) design has been changed for satellites F6 & F7 which changed the DDI output line (SSIEDAT) characteristics as shown in Figure 2-6. For satellites F2, F4, and F5, data is transfered once per second upon receiving the read pulse (SSIERED) of 180mS in duration from the OLS which allows the data storage registers to shift out data acquired during the 1 sec. period prior to the end of the read period. The Least Significant Bit (LSB) of Word 1 is shifted out first with the data block shifting out serially at a $1\,KH_z$ rate. For F6 and F7, the SSIERED pulse is 18mS with the data block shifting out at a $10\,KH_z$ rate. Table 2-2 shows the status of the 5 flight units as of 31 MAY 80.

Ten trips were made to RCA, Hightstown, N.J., in support of the DMSP Satellite Program which included integration tests, stand alone tests, GO-NO GO tests and final inspections. Also, 2 trips were made to Vandenberg AFB for preflight GO-NO GO tests for the F4 and F5 satellites.

(b) The objective of the DMSP follow-on SSIES Plasma Monitor is also to obtain critical information about the characteristics of the space plasma above the peak of the F region. Data will be obtained from four electrostatic probes similar to those for the SSIE with the addition of instrumentation for a Drift/Scintillation Monitor. The SSIES will be flown on a series of DMSP Block 5D-2 Satellites commencing with the F8 launch. The main features of the (SSIES) system are shown in Figure 2-5 Block Diagram. Control grids within the Electron and Ion Sensors are biased and periodically swept through small voltage ranges to determine the temperature and density of the particles collected. In order to produce meaningful data, these grids must be biased at a DC

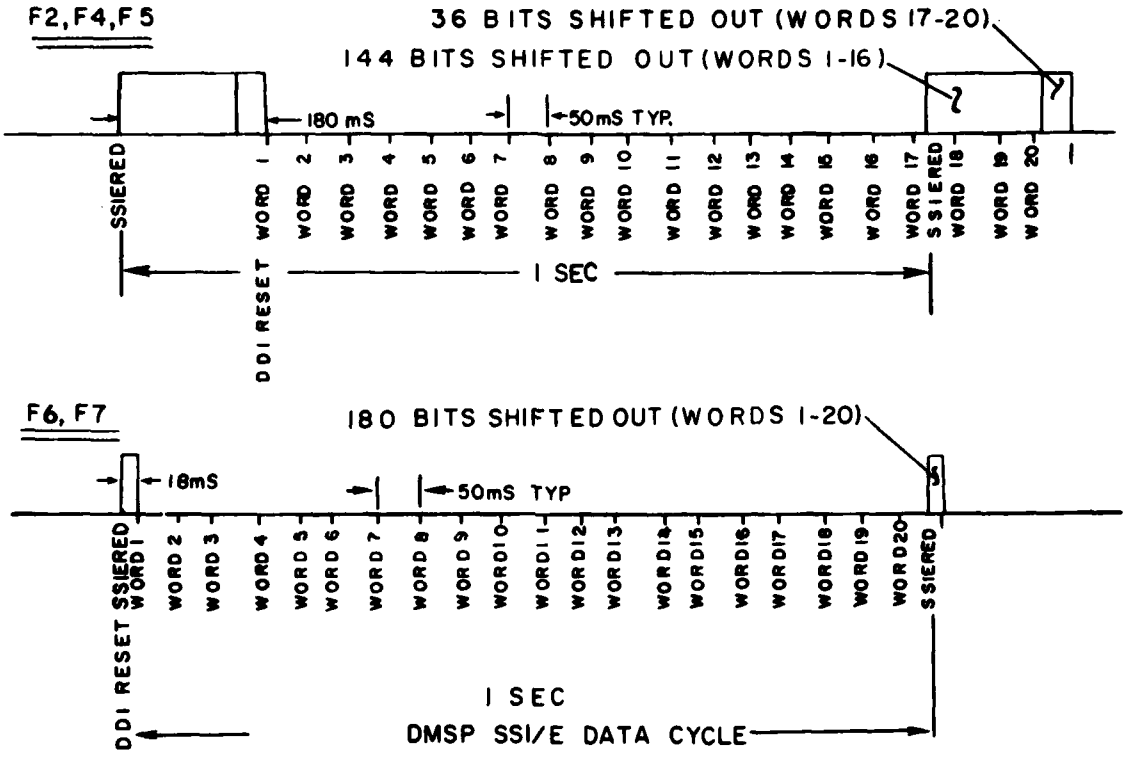

Figure 2-6: DMSP SSI/E Data Cycle for F2 through F7

Table 2-2

STATUS OF SSI/E ELECTRONIC PACKAGES

DMSP SATELLITE SSI/E PACKAGE	F2 S/N 1	F4 S/N 3	F5 S/N 4	F6 S/N 5	F7 S/N 2
ASSEMBLED	X	X	X	X	X
AUX. POWER SUPPLY	NA	X	X	X	X
SSIEDAT - 1 KH_z	X	X	X	NA	NA
SSIEDAT - 10 KH_z	NA	NA	X	X	X
BURN - IN	X	X	X	X	X
CALIBRATED	X	X	X	X	
RCA INTEGRATION	X	X	X		
VIBRATION TESTS	X	X	X		
THERMAL - VACUUM	X	X	X		
ACOUSTICS TEST	X	X	X		
STAND ALONE	X	X	X		
VANDENBERG GO-NO GO	X	X	X		
LAUNCHED	X	X	FAILED		

potential somewhere near that of the spacecraft. These bias potentials are determined by analysis of the data on the ground and set by ground command and under certain operating modes, the electronics package will determine and set the bias potentials automatically. The various bias and sweep circuits and their relation to one another are also shown in Figure 2-8. In addition, the main electronics will analyze the sweep data from both sensors and calculate the density and temperature of the detected electrons, Hydrogen ions and Oxygen ions. At all times the raw sensor output will be transmitted to ground for verification of on-board calculations.

Complete design specifications were developed for the SSIES Electronics Package during this contract reporting period. The Electronics Package Configuration, Figure 2-9, shows the connector locations that interface with other spacecraft assemblies and the packaging of the circuitry by the various printed boards. The electronics package interfaces with Operational Linescan System (provides data processing signals and receives data from SSIES), Sensors (interfaces planar Ion sensor and spherical Electron sensor), Drift/Scintillation Monitor (interface connections with drift and scintillation experiment) and Spacecraft (provides primary power from spacecraft).

The controlling element of the SSIES Electrons Package will be a microprocessor (SBP9900A) manufactured by Texas Instruments. Several microprocessors were evaluated with the majority being implemented in the NMOS, PMOS, and CMOS technologies. None of these devices exhibit the required radiation resistance required (10^5Rads) nor are they available in a hardened version. The SBP9900A is manufactured using the I^2L technology which is radiation hardened by nature and is also available screened to M38510 specifications. The processor has a 16 bit architecture which allows high resolution arithmetic and is compatible

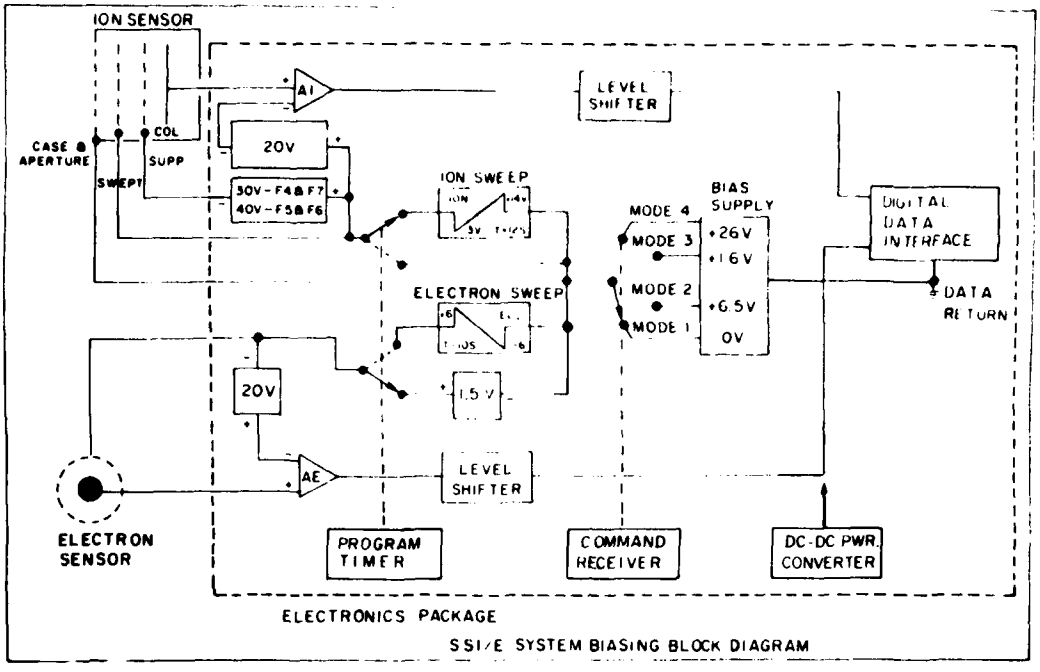

Figure 2-8: SSI/E System Biasing Block Diagram

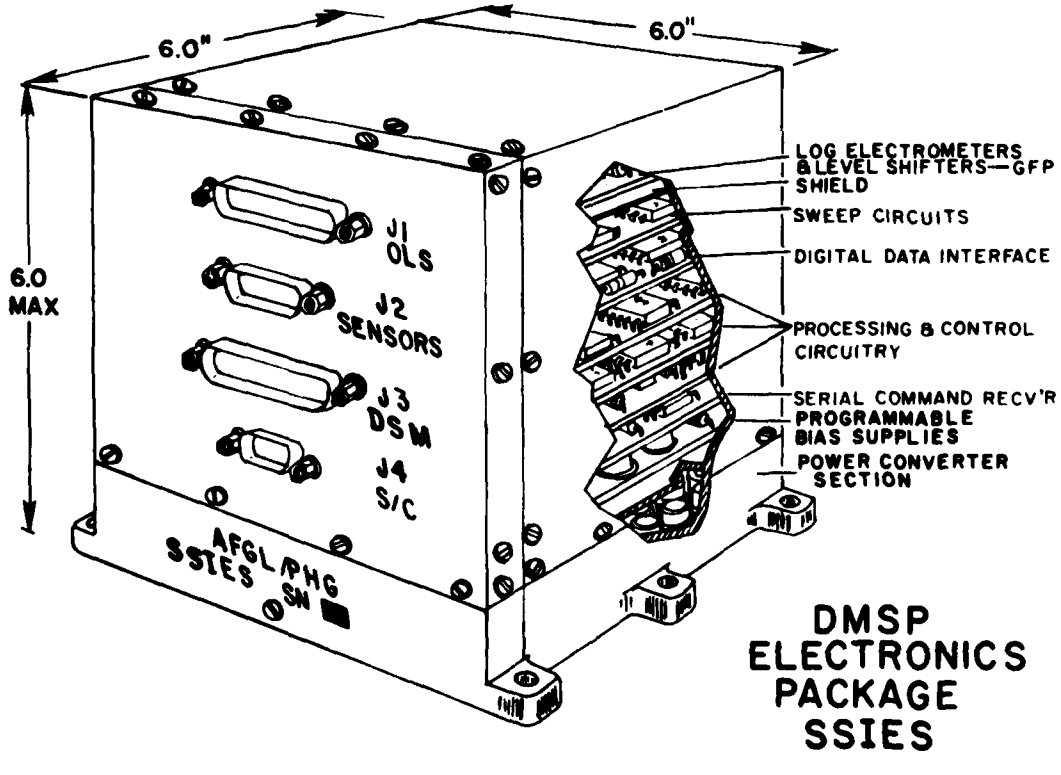

Figure 2-9: DMSP Electronics Package SSIES

with the 9 bit data format. The processor will be driven by a fail-safe oscillator circuit at speeds which will allow for margins for any possible radiation induced speed degradation. The processor will use an array of random access memory (RAM) and programmable read-only memory (PROM) which interfaces the processor's memory address and data busses. All program cycle and mode operations will be under computer control implemented using input and output operations utilizing the processor's communications register unit (CRU) bus. The CRU bus, in turn, communicates with other sub-systems within the electronics package, using addressable latches and data selectors as I/O interface devices. The address latches allow control outputs from the processor to be latched providing control signals to the different devices controlled by the processor system. A data selector will interface the reading of data from external systems into the processor system.

Ground commands are processed by the OLS unit which generates serial command signals (SSIESSER) for the Electronics Package thru the OLS connector interface as shown in Figure 2-8. The serial command assignments are shown in Tables 2-3 & 2-4. Serial commands will be buffered into a serial buffer register, which accepts the 8 bit commands and then will generate a command received interrupt signal to the processor. The processor will then read the 8 bit command through the data selector interface.

Another OLS timing signal designated SSIESREF will be used as the system primary clock. It will drive the system timing chain and real time clock circuitry which in turn generates the timing required for the processor's real time clock interrupt, the analog to digital converter (A/D) synchronization gate (which allows precise timing of the analog to digital conversion samples), the Ionosonde timing pulse required to disable it when the electron

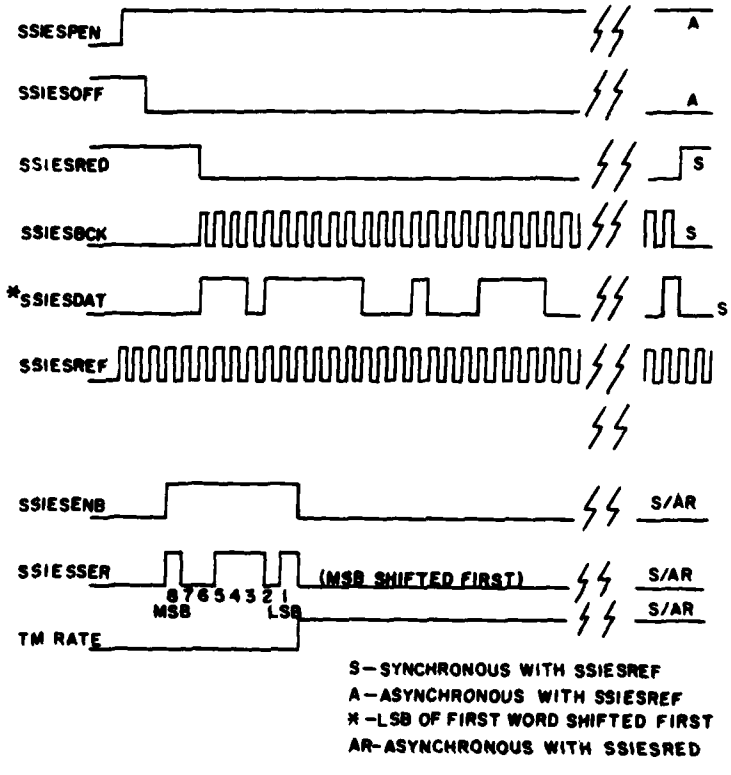

Figure 2-10: OLS Timing Diagram

TABLE 2-3

SSIES SERIAL COMMAND ASSIGNMENTS

SERIAL COMMAND		SSIES INTERNAL COMMAND INTERFACE		
BINARY 8 7 6 5 4 3 2 1	HEXADECIMAL 21	ADDRESS 8 7 6 5	DATA 4 3 2 1	FUNCTION
0 0 0 1 0 0 0 0	10	0 0 0 1	0 0 0 0	PROGRAM RESET-SWEEP CYCLES
0 0 0 1 0 0 0 1	11	0 0 0 1	0 0 0 1	MODE A
0 0 0 1 0 0 1 0	12	0 0 0 1	0 0 1 0	MODE B
0 0 0 1 0 0 1 1	13	0 0 0 1	0 0 1 1	MODE C
0 0 0 1 0 1 0 0	14	0 0 0 1	0 1 0 0	MODE D
0 0 0 1 0 1 0 1	15	0 0 0 1	0 1 0 1	MODE E
0 0 0 1 0 1 1 0	16	0 0 0 1	0 1 1 0	STEP V_{BIAS} By + 1V.
0 0 0 1 0 1 1 1	17	0 0 0 1	0 1 1 1	STEP V_{BIAS} By - 1V.
0 0 0 1 1 0 0 0	18	0 0 0 1	1 0 0 0	STEP V_{BIAS} By + 2V.
0 0 0 1 1 0 0 1	19	0 0 0 1	1 0 0 1	STEP V_{BIAS} By - 2V.
0 0 0 1 1 0 1 0	1A	0 0 0 1	1 0 1 0	STEP V_{BIAS} By + 4V.
0 0 0 1 1 0 1 1	1B	0 0 0 1	1 0 1 1	STEP V_{BIAS} By - 4V.
0 0 0 1 1 1 0 0	1C	0 0 0 1	1 1 0 0	STEP V_{IP} By + 1V.
0 0 0 1 1 1 0 1	1D	0 0 0 1	1 1 0 1	STEP V_{IP} By - 1V.
0 0 0 1 1 1 1 0	1E	0 0 0 1	1 1 1 0	CLOCK ON-SWEEPS ONLY
0 0 0 1 1 1 1 1	1F	0 0 0 1	1 1 1 1	CLOCK OFF-SWEEPS ONLY
0 0 1 0 0 0 0 0	20	0 0 1 0	0 0 0 0	SPARE
0 0 1 0 0 0 0 1	21	0 0 1 0	0 0 0 1	SPARE
0 0 1 0 0 0 1 0	22	0 0 1 0	0 0 1 0	SPARE
0 0 1 0 0 0 1 1	23	0 0 1 0	0 0 1 1	SPARE
0 0 1 0 0 1 0 0	24	0 0 1 0	0 1 0 0	
0 0 1 0 0 1 0 1	25	0 0 1 0	0 1 0 1	
0 0 1 0 0 1 1 0	26	0 0 1 0	0 1 1 0	
0 0 1 0 0 1 1 1	27	0 0 1 0	0 1 1 1	
0 0 1 0 1 0 0 0	28	0 0 1 0	1 0 0 0	
0 0 1 0 1 0 0 1	29	0 0 1 0	1 0 0 1	
0 0 1 0 1 0 1 0	2A	0 0 1 0	1 0 1 0	
0 0 1 0 1 0 1 1	2B	0 0 1 0	1 0 1 1	
0 0 1 0 1 1 0 0	2C	0 0 1 0	1 1 0 0	
0 0 1 0 1 1 0 1	2D	0 0 1 0	1 1 0 1	
0 0 1 0 1 1 1 0	2E	0 0 1 0	1 1 1 0	
0 0 1 0 1 1 1 1	2F	0 0 1 0	1 1 1 1	

TABLE 2-4

DSM SERIAL COMMAND ASSIGNMENTS

SERIAL COMMAND		SSIES INTERNAL COMMAND INTERFACE		
BINARY 8 7 6 5 4 3 2 1	HEXADECIMAL 21	ADDRESS 8 7 6 5	DATA 4 3 2 1	FUNCTION
0 0 1 1 0 0 0 0	30	0 0 1 1	0 0 0 0	DRP 1
0 0 1 1 0 0 0 1	31	0 0 1 1	0 0 0 1	DRP 2
0 0 1 1 0 0 1 0	32	0 0 1 1	0 0 1 0	DRP 3
0 0 1 1 0 0 1 1	33	0 0 1 1	0 0 1 1	DRP 4
0 0 1 1 0 1 0 0	34	0 0 1 1	0 1 0 0	DRP 5
0 0 1 1 0 1 0 1	35	0 0 1 1	0 1 0 1	DRP 6
0 0 1 1 0 1 1 0	36	0 0 1 1	0 1 1 0	DRP 7
0 0 1 1 0 1 1 1	37	0 0 1 1	0 1 1 1	DRP 8
0 0 1 1 1 0 0 0	38	0 0 1 1	1 0 0 0	Spare
0 0 1 1 1 0 0 1	39	0 0 1 1	1 0 0 1	Spare
0 0 1 1 1 0 1 0	3A	0 0 1 1	1 0 1 0	
0 0 1 1 1 0 1 1	3B	0 0 1 1	1 0 1 1	
0 0 1 1 1 1 0 0	3C	0 0 1 1	1 1 0 0	
0 0 1 1 1 1 0 1	3D	0 0 1 1	1 1 0 1	
0 0 1 1 1 1 1 0	3E	0 0 1 1	1 1 1 0	
0 0 1 1 1 1 1 1	3F	0 0 1 1	1 1 1 1	
0 1 0 0 0 0 0 0	40	0 1 0 0	0 0 0 0	FBR Enable all Filters
0 1 0 0 0 0 0 1	41	0 1 0 0	0 0 0 1	FBR Disable F1
0 1 0 0 0 0 1 0	42	0 1 0 0	0 0 1 0	FBR Disable F2
0 1 0 0 0 0 1 1	43	0 1 0 0	0 0 1 1	FBR Disable F3
0 1 0 0 0 1 0 0	44	0 1 0 0	0 1 0 0	FBR Disable F4
0 1 0 0 0 1 0 1	45	0 1 0 0	0 1 0 1	FBR Disable F5
0 1 0 0 0 1 1 0	46	0 1 0 0	0 1 1 0	FBR Disable F6
0 1 0 0 0 1 1 1	47	0 1 0 0	0 1 1 1	FBR Disable F7, F8, F9
0 1 0 0 1 0 0 0	48	0 1 0 0	1 0 0 0	FBR Enable F7, F8, F9
0 1 0 0 1 0 0 1	49	0 1 0 0	1 0 0 1	FBR Disable F7
0 1 0 0 1 0 1 0	4A	0 1 0 0	1 0 1 0	FBR Disable F8
0 1 0 0 1 0 1 1	4B	0 1 0 0	1 0 1 1	FBR Disable F7, F8
0 1 0 0 1 1 0 0	4C	0 1 0 0	1 1 0 0	FBR Disable F9
0 1 0 0 1 1 0 1	4D	0 1 0 0	1 1 0 1	FBR Disable F7, F9
0 1 0 0 1 1 1 0	4E	0 1 0 0	1 1 1 0	FBR Disable F8, F9
0 1 0 0 1 1 1 1	4F	0 1 0 0	1 1 1 1	

bias establishes sweeps are present, and finally, the SSIESRED interrupt which is the primary synchronizing signal used by the processor.

The SSIES Electronics Package receives data signals from the Ion and Electron sensors which are connected to Log electrometers amplifiers. These output signals are digitized by the A/D circuitry along with other data signals received from the DSM experiment. The processor formats the data sampling sequence as shown in Figure 2-11 which stores the data in RAM devices for the downlink serializer. The downlink serializer will be used to buffer and serialize the accumulated data (SSIESDAT) during its burst of shifting pulses (SSIESBCK), when gated (SSIESRED), to the OLS.

The DSM interface circuits buffer uplink control addresses to the DSM through the address latches and provide the data input path for sampling by the A/D circuitry. Address latch interfaces will also be used to provide the control signals for both the electron and Ion sweep generators which are shown in Figure 2-12. The design provides digital sweep signals which are controlled by the processor. The processor will determine whether the sweep will have a negative or positive slope, a 20 volt or 6 volt magnitude, a reset to zero volts interval, and timing periods of 2, 3, or 4 seconds. The timing periods will also be used for initiating several calculations which are to be performed at the end of each sweep period. Lookup tables stored in the PROM devices will be used by the processor in calculating these unknowns.

A DC to DC power converter will provide the many secondary circuits and bias voltages for the Electronics Package, DSM experiment, and sensors. The design estimate of the processor's on time indicates that it will need power for

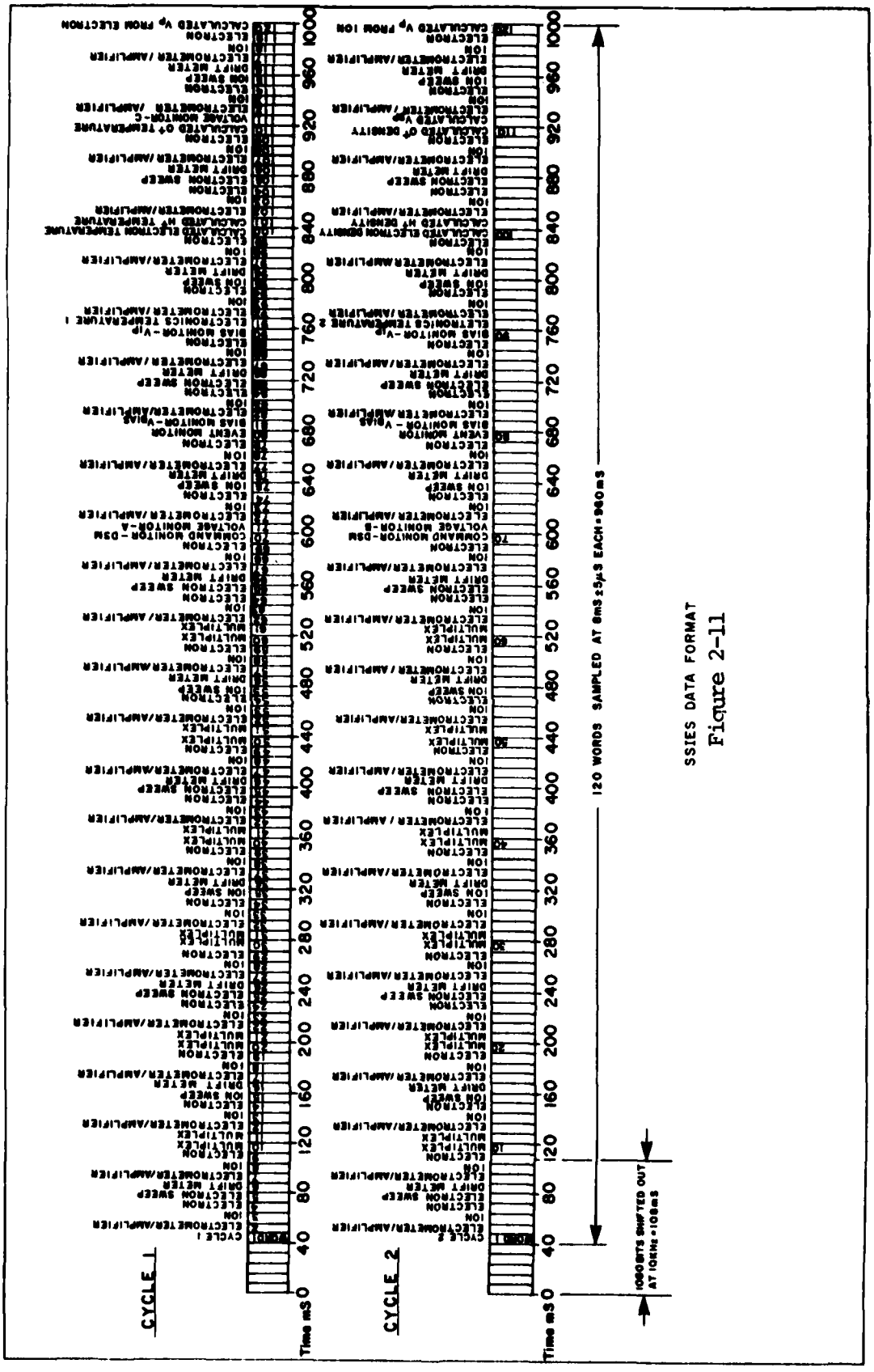
CYCLE 1
CYCLE 2
Time mS
0
40
80
120
160
200
240
280
320
360
400
440
480
520
560
600
640
680
720
760
800
840
880
920
960
1000
120 WORDS SAMPLED AT 8mS±5μS EACH = 960mS
1080 BITS SHIFTED OUT AT 10KHz = 108mS
SSIES DATA FORMAT

Figure 2-11

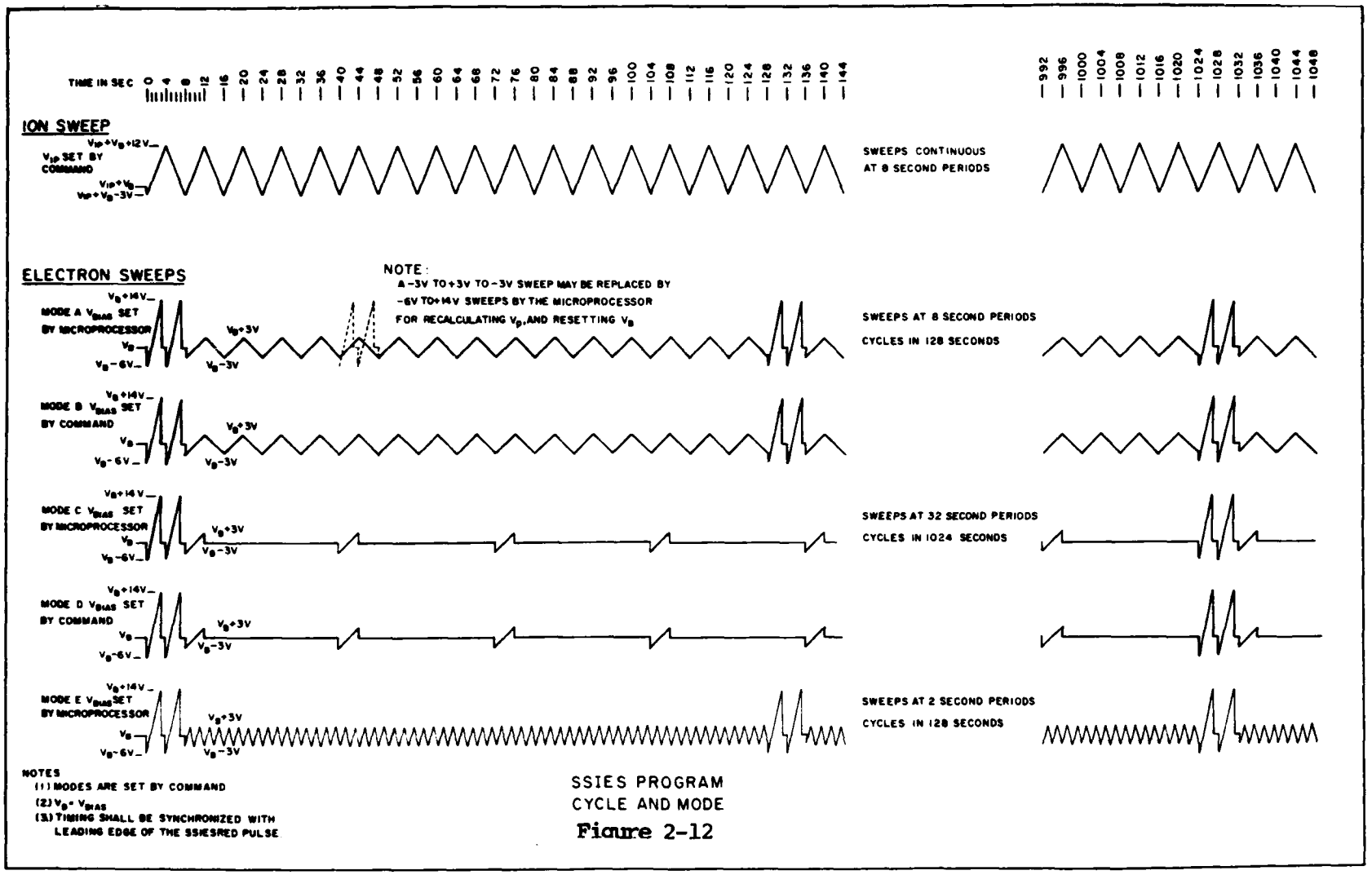

SSIES PROGRAM
CYCLE AND MODE

Figure 2-12

less than 10% of the time. This means that the processor and memory devices can be power strobed which will conserve power. Also, this will provide high reliability and longer expected life.

Two trips were made during this contract for interface meetings. One was made to the University of Texas at Dallas and the other to RCA, Highstown, N.J.

4. AURORAL - E ROCKET (A10.903)

Four rocket payloads will be launched from Poker Flat Alaska during the next contract period as part of the Auroral-E Program to obtain in-situ measurements of several atmospheric and ionospheric parameters during a continuous aurora. The goals of the rocket program are nearly simultaneous measurements of the energy and angular distribution of electron and proton flux, optical emissions from atomic and molecular atmospheric constituents, ion species, electron densities, neutral and mass densities, neutral and electron temperatures, neutral winds and electric fields. The rocket measurements will be coordinated with the pass of a satellite which will measure precipitating electrons and protons. The AFGL Airborne Ionospheric Observatory will be positioned near the rocket launch site and will measure auroral optical emissions as well as ionospheric parameters. In addition, ground based measurements of electron density profiles in the region of the rocket trajectories will be measured with incoherent scatter radar at Chatanika.

The system to be used for measuring the electric fields was designed under this contract and the flight components of the E-Field System are shown in Figure 2-13. The objective of the E-Field experiment is to measure the elec-

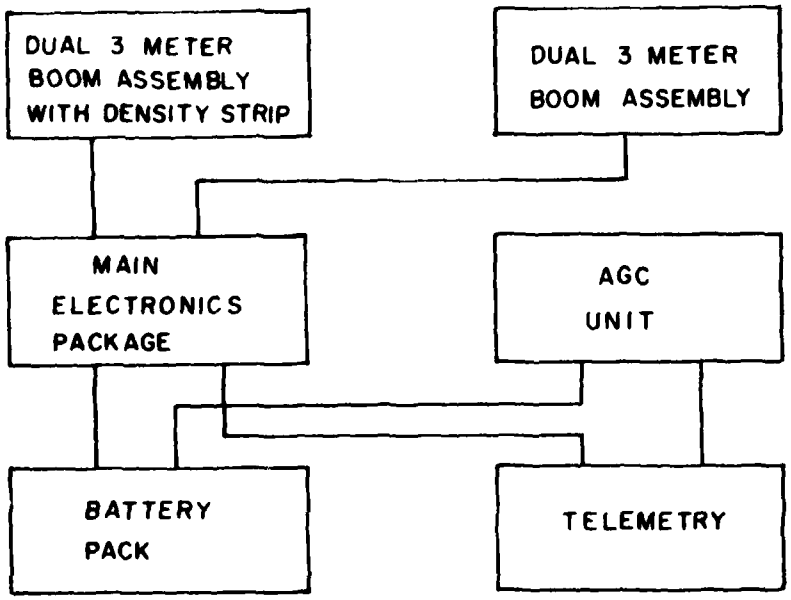

Figure 2-13: E - Field Block Diagram Auroral -E Rocket

tric field as a function of altitude for the continuous aurora. The method of measurement is to deploy two mutually perpendicular dipoles normal to the rocket spin axis, separated by a large fore and aft distance. The mutual potential differences between pairs of spherical sensors mounted at the dipole tips, with a 3 meter separation, will yield a vector electric field measurement. The field will be measured in the frequency range of 0 to 100 H_z, from -100 mV/m to +100 mV/m, to an accuracy of $\pm$0.5 mV/m.

With the above circuitry designed, development of the flight system will continue on the follow on contract. These circuits will be designed onto printed circuit boards after the breadboard phase has been completed at AFGL. The circuitry includes a DC to DC power supply, Log electrometer for the Density measurement, 4 electric field electrometer amplifiers, difference amplifiers, and Butterworth filters.

5. CONTINUING EDUCATION

Four separate courses were attended during this contract reporting period. One was for "Designing for Reliability" which was held in Hempstead, NY. Another course "Managing Engineers" was attended in Chicago, IL. The other two courses were held at the Boston office of Tektronix Corp. One course was for a "Microprocessor Design Workshop" and the other for "Microprocessor Lab Operations".

III.

SCIENTIFIC DATA ANALYSIS OF SATELLITE MEASUREMENTS OF THERMAL PLASMA, ELECTRIC FIELDS AND MAGNETIC FIELDS

Frederick J. Rich, Ph.D.

1. Analysis and Interpretation of S3-2 Data

The S3-2 satellite was put into a polar orbit of 240 km by 1550 km in December, 1975 and it re-entered the atmosphere in May, 1978. It carried instruments from the Air Force Geophysics Laboratory to measure thermal ion density and drift velocity, thermal electron density and temperature, energetic electrons in the range of 0.1 to 20 keV, the in-situ electric field, and the magnetic field. This complement of instruments has been described in publication #36 under this contract.

From a combination of the data sets from the S3-2 satellite, it is possible to get an instantaneous description of the state of the ionosphere near the satellite. This is especially true at high latitudes where the ionosphere is strongly affected by energetic particles and electric fields that are generated in the magnetosphere and solar wind above the ionosphere. From these recordings of the state of the ionosphere it is possible to find clues about how and why the ionosphere changes in response to changes in the magnetosphere, the solar wind and the sunspot cycle. This contract has undertaken studies to learn more about these interactions, but a complete understanding has eluded us and will elude the entire scientific community for years to come because the ionosphere is complex and constantly changing.

Since a vast array of observations around the globe cannot be made simultaneously, it will be necessary to compile and compare a vast array of observations taken around the globe under similar circumstances in order to understand the ionosphere.

1.1 Intense Convection in the Sub-auroral Region

From previous measurements, it was known that an electric field existed in the auroral zone, especially during geomagnetically disturbed times. This electric field at the altitude of the S3-2 satellite generally has a strength of a few millivolts/meter during quiet times and a strength of 20 - 50 mV/m during disturbed times. The direction of the electric field is such that the $\underline{E} \times \underline{B}$ drift of the ionosphere is approximately sunward along a constant latitude between 60° and 72° in magnetic coordinates. In publication number 7, we reported a case of greatly enhanced strength of the electric field (approximately 250 mV/m) near the equatorward boundary of the auroral zone. Figure 3-1 shows the electric field and the magnetic field deflection for the first case found and reported upon. The electric field shown represents 5 second averages of the data. Changes in the magnetic field deflection represent currents flowing along magnetic field lines either into or out of the ionosphere.

The existence of a strong electric field near the equatorward edge of the auroral zone was quite surprising. Generally the strongest electric field in the auroral zone is near the poleward edge of the zone near the region of discrete arcs and the auroral electrojet. The auroral electrojet is caused by Hall currents flowing between 100 and 150 km altitude. The Hall current is dependent upon the existence of a strong electric field, field aligned currents

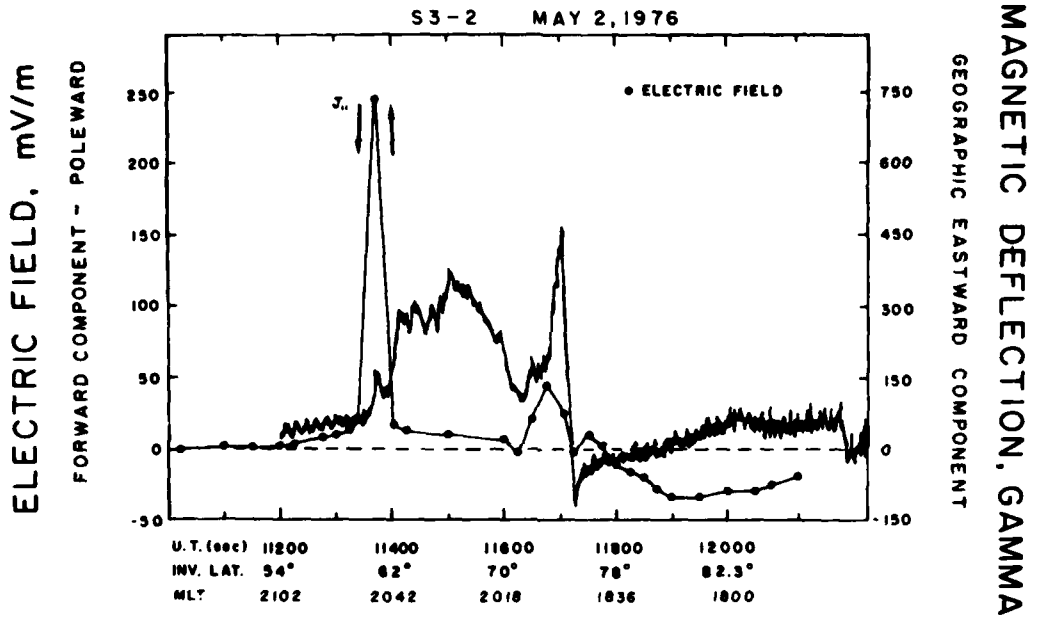

Figure 3-1: The measured electric field and magnetic field deflection from S3-2 from mid-latitude through the auroral zone to the polar cap.

on either side of it and high levels of ionization at low altitudes due to either sunlight or bombardment of energetic particles from the magnetosphere. In Figure 3-1, two of these three conditions are observed between 70° and 74° invariant latitude which is typical of the auroral zone during active times.

Since the auroral electrojet can be observed from the ground with magnetometers, the existence of strong electric fields and field aligned currents near the poleward edge of the auroral zone was suggested before direct observations were made. Since electrojets on the equatorward edge of the auroral zone have not been observed, it is possible that there is insufficient ionization in the low altitude ionosphere for a Hall current to flow when a very strong electric field exists. In order to better understand the nature of these very strong electric fields on the equatorward boundary of the auroral zone, further research was undertaken which resulted in publication numbers 22 and 37. Figure 3-2 shows further details of the same data set shown in Figure 3-1.

The results of this further study showthat there should be currents flowing in the altitude ionosphere near these very strong electric fields, but ground based observations may be unreported because these events are relatively rare. From Figure 3-2, we can see that there are some precipitating energetic particles (bottom trace on the figure) although the flux is weak. Also there are field aligned currents near the strong electric field. Thus the conditions for a Hall current do exist although it may not be as strong as the auroral electrojet on the poleward edge of the auroral zone. Also, we could find only seven cases of very strong electric fields ($E > 100\,mV/m$) in the first nine months of data taken. Thus these very strong electric fields

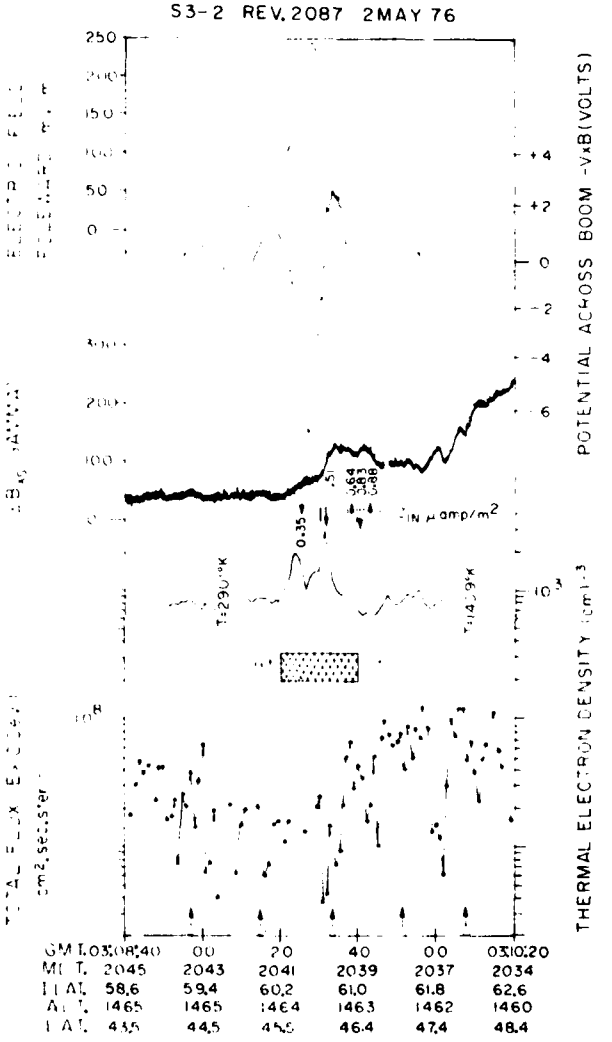

Figure 3-2: An expanded view of the data from Figure 3-1 in the region of the very intense electric field on the equatorward boundary of the auroral zone. The raw electric field, the despun electric field, the magnetometer deflections, the thermal electron density and the flux of energetic electrons are shown.

do not occur very often. However strong electric fields ($20 < E < 100$ mV/m) on the equatorward edge of the auroral zone are more common as determined by Spiro et al. of Univ. of Texas at Dallas using Atmospheric Explorer data. If these strong electric fields have the same source as the very strong electric field, then the source of the electric field is a reasonably common phenomenon. In our research, we suggest that the strong or very strong electric field at the equatorward edge of the auroral zone is caused by charge separation at the inner edge of the plasmasheet as the plasmasheet is pushed earthward during the growth and expansion phases of a substorm. The strength of the electric field is determined by the degree of violence with which the plasmasheet is pushed earthward.

1.2 Electrodynamics of Visible Auroral Arcs

Auroral physics has been driven during the past century by the desire to understand the visible aurora despite the knowledge gained during the space age which indicates that the visible aurora is a small part of a vast and complex mechanism. Thus we have undertaken to relate all of the parameters available from the S3-2 data set to a visible aurora. This work was reported in publications 27 and 36. Orbit 517 on 11 January 76 was used for this study because an optical image of an auroral display was made by the DMSP satellite within a few minutes of the passage of the S3-2 satellite (Figure 3-3). A survey of the S3-2 data for this period (Figures 3-4 and 3-5) shows a typical passage through the auroral zone. There is a significant density enhancement, electric field and particle precipitation throughout the auroral zone, but they are all strongest on the poleward edge of the auroral zone. The equatorward section of the auroral zone is dominated by downward currents

FIGURE 3-3: DMSP image of the auroral region on 11 January 1976, ~14 minute prior to the passage of S3-2 (dashed line).

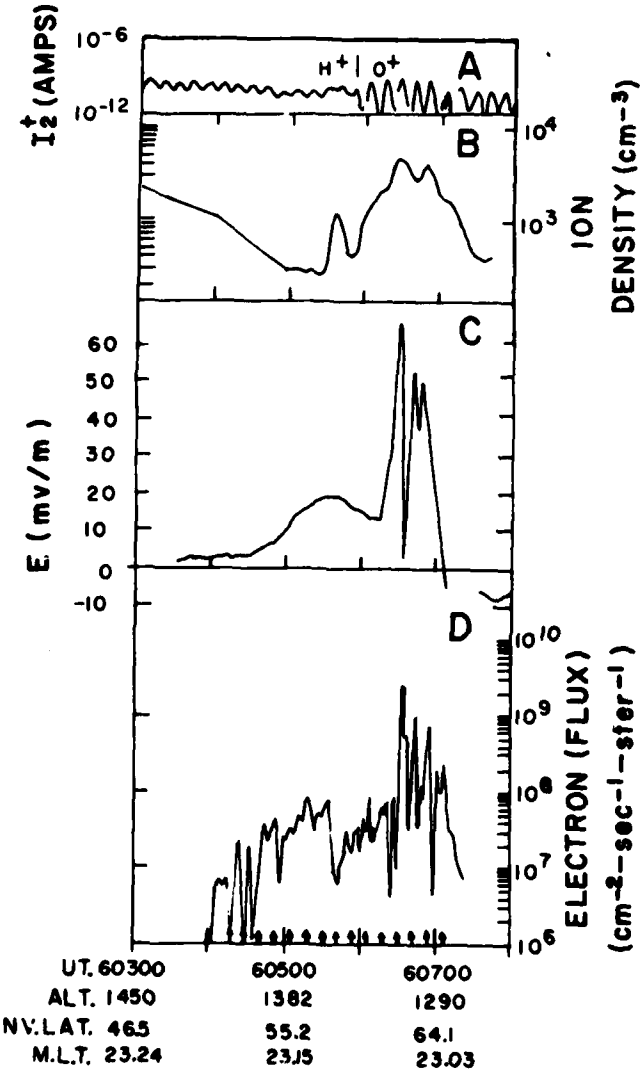

FIGURE 3-4: Simultaneous measurements from S3-2 ion trap, electric field experiment and energetic electron experiment.

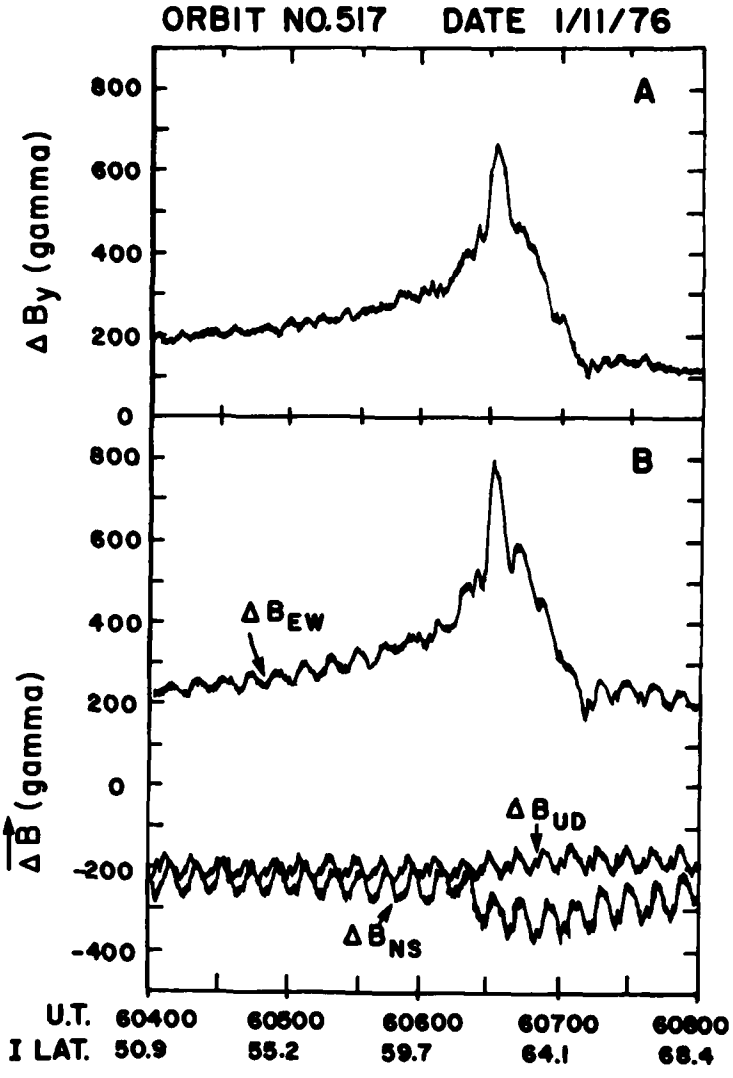

FIGURE 3-5: Measured magnetometer deflection along the axis of the S3-2 satellite and in geomagnetic coordinates. The spin modulation of the geomagnetic coordinate data is a residue of a mis-match of the axes of the instrument.

along the field lines (positive slopes in ΔB_y or ΔB_{EW}). The poleward section is dominated by upward currents (negative slopes in ΔB_y or ΔB_{EW}).

From these surveys of the data, the location of the visible aurora is not apparent. It is necessary to compare the location of the visible aurora in Figure 3-3 with the data shown in Figures 3-4 and 3-5 to find which features are directly related to the visible aurora. The dashed line in Figure 3-3 shows the ground track of 33-2 satellite. If one traces the magnetic field lines from the satellite to the altitude of the visible aurora, the auroral arc slightly eastward of the ground track is the appropriate section of the aurora to compare with the satellite data. The visible, discrete arc of interest lies near 62° - 63° invariant latitude. Equatorward of the discrete arc is a region of diffuse aurora. The diffuse aurora corresponds to a region of generally downward current, and the discrete aurora corresponds to a region of generally upward current. Figures 3-6 and 3-7 show the data in more detail. In the diffuse auroral region (Figure 3-6) despite the general downward flow of field aligned current, there are regions of upward current caused by downward flowing energetic electrons which exceed the flux of upward flowing thermal electrons. These regions of upward current are labelled 1 through 4 on Figure 3-6. The drops in the thermal electron current in these regions is caused by the vehicle potential becoming negative which repells thermal electrons away from the vehicle. In the region of the discrete aurora (Figure 3-7) there are three regions of strong upward current followed by weak upward current or downward current. These three regions are labelled 1 through 3 in Figure 3-7. In the region of electric field strength is decreased from the five second average (smooth curve with dots) and the flux of energetic electrons is increased (if the detector was looking in the proper direction).

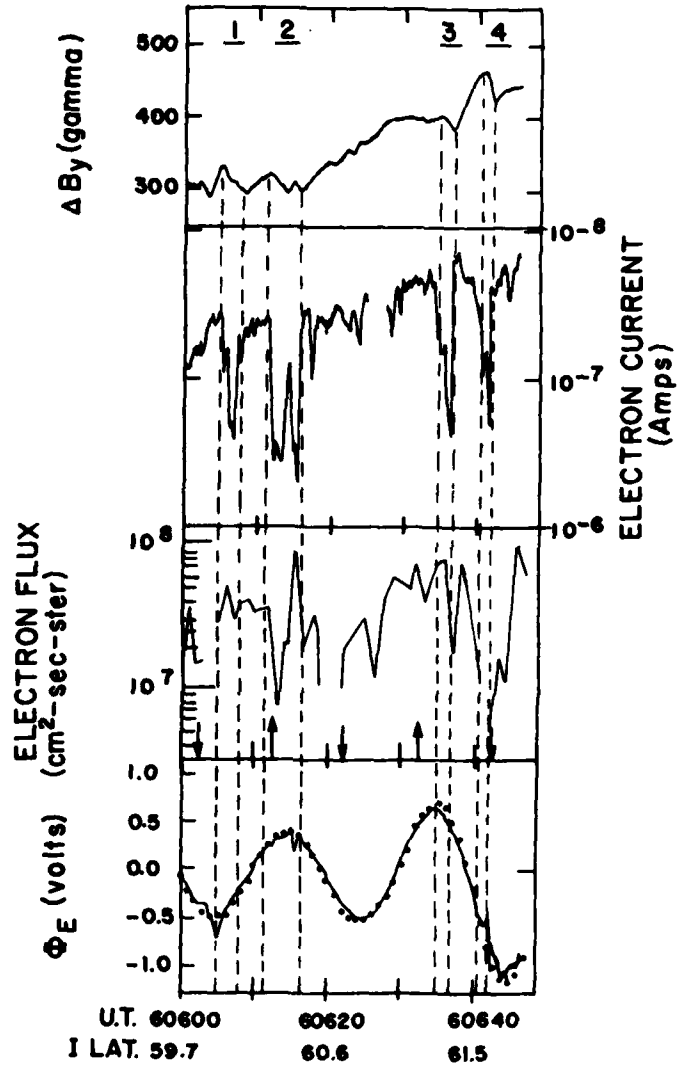

FIGURE 3-6: High time resolution of ΔB_y, the current to the thermal electron probe and the energetic electron directional flux in the equatorward or Region 2 portion of the auroral zone.

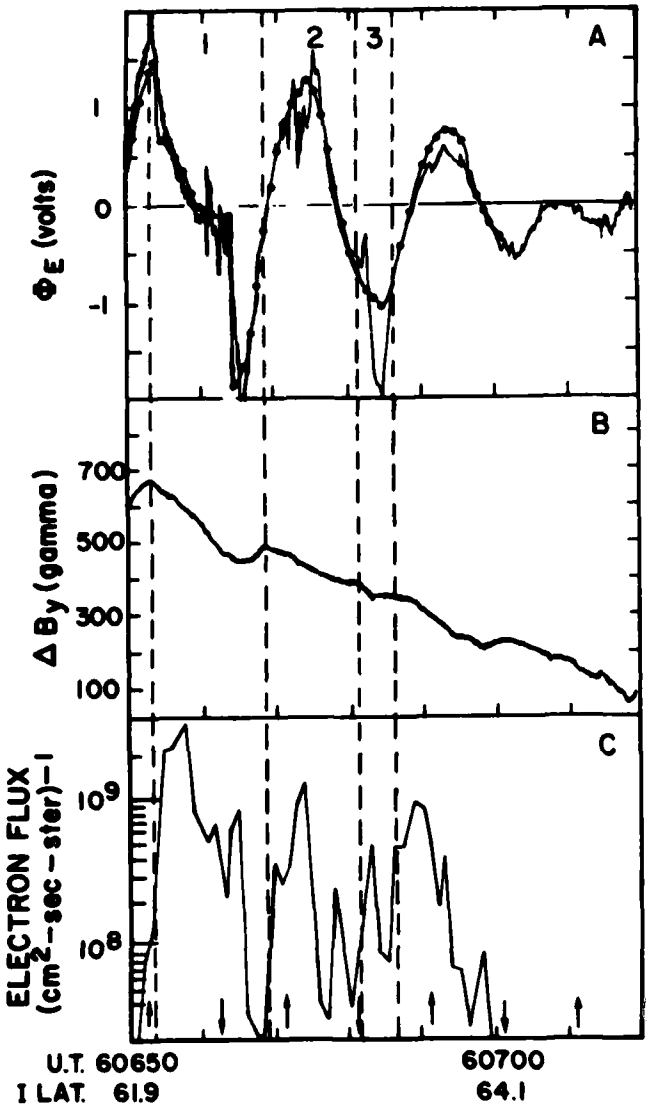

FIGURE 3-7: Same as Figure 3-6 except that the data is taken from the poleward or Region 1 portion of the auroral zone.

There should be three arcs in the photograph of the aurora along the track of the satellite (Figure 3-3). An analysis of the slope of the magnetic field lines with respect to the position of the DMSP satellite indicates that the arcs labelled 1 and 2 in Figure 3-7 will overlap in the photograph if they have a visible vertical extent of ~100 km. The arc labelled 3 in Figure 3-7 is probably not strong enough to produce a visible auroral display. In summary, the visible auroral arcs represent part of the region of upward current, but most of the upward current flows outside of the region of visible auroral arcs.

1.3 The Convection Electric Field in the Polar Cap

The sunward convection of ionospheric plasma has generally been described as one half of a convection pattern. The other half is the anti-sunward convection across the polar cap. In publications number 16 and 17, we investigated the convection patterns in the polar cap regions using the electric field experiment from S3-2. We found that during times of moderate to intense geomagnetic activity, the convection is clearly anti-sunward as indicated by previous investigators but that it is not uniformly distributed across the polar cap. Often, convection is stronger on the dawn or dusk flank than it is on the opposite flank and this asymmetry across the northern polar cap is opposite to the asymmetry of convection across the southern polar cap at the same time. This can be explained by comparing the asymmetry of convection in the polar cap with the magnitude of the "y" component, or dusk-dawn component, of the interplanetary magnetic field. Apparently when there is a significant B_y component of the IMF, the magnetic tension between geomagnetic field lines connected to interplanetary magnetic field lines pulls the field lines

toward opposite flanks of the magnetosphere. By tracing these field lines into the ionosphere, the same forces pull convection to opposite flanks of the polar cap.

Most geomagnetic activity occurs when the "z" component of the interplanetary magnetic field is southward or almost zero. Under such conditions, geomagnetic field lines on the front side of the magnetosphere merge with the IMF and energy is transferred from the solar wind to the magnetosphere. When the B_z component of the IMF is northward, there is less geomagnetic activity due to less energy transfer into the magnetosphere and the high latitude convection pattern become weak and/or irregular. We investigated some of the irregular convection patterns and found that there is a regularity to them although it is not the standard two cell convection pattern. Figure 3-8 shows an example of the forward or dawn-dusk component of the electric field and the convection pattern implied by the convection directions observed along the path of the satellite. Here we have a four cell convection pattern. The energy for this motion comes from the solar wind through merging of geomagnetic field lines with the IMF. However, instead of merging occurring at the front of the magnetosphere, it occurs at the high latitude regions of the magnetosphere.

2. Analysis and Interpretation of S3-3 Data

The S3-3 satellite was put into a polar orbit of 240 by 8050 km in July, 1976 and it continued to function properly until September, 1979. It carried instruments from the Air Force Geophysics Laboratory to measure thermal ion density and drift velocity and thermal electron density and temperature. Energetic particles, electric field and magnetic fields were measured by instru-

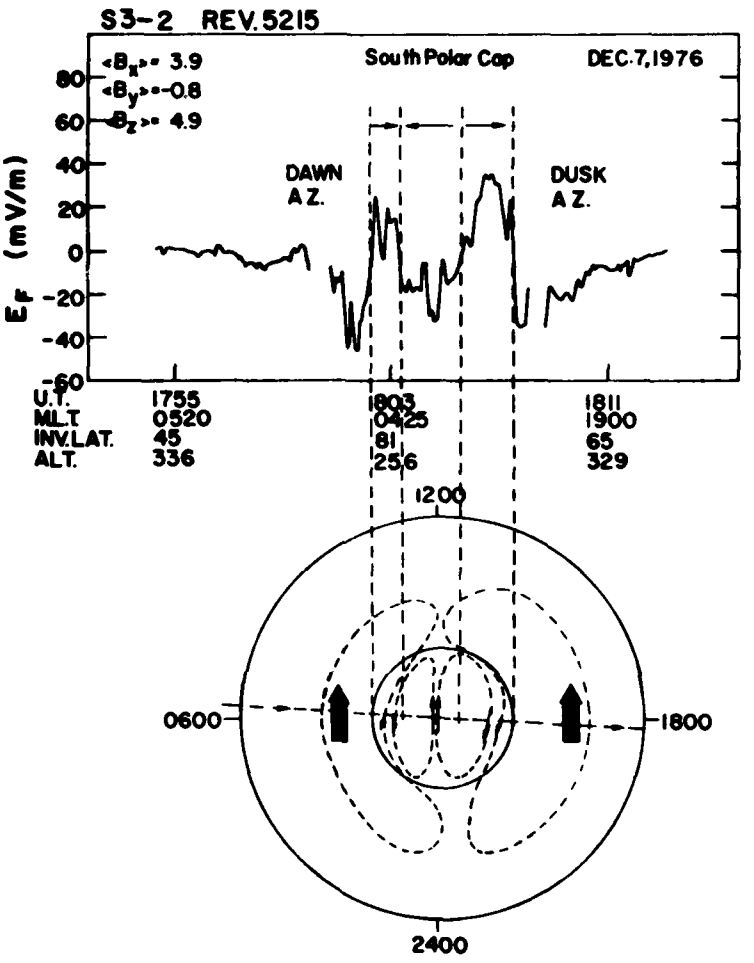

FIGURE 3-8: The measured electric field across the polar cap and the proposed convection pattern during a period of northward directed IMF and sunward convection in the polar cap.

ments provided by Aerospace Corp., Lockheed Corp. and Univ. of California, Berkeley. Results from the ion sensor has previously been reported upon in Technical Report AFGL-TR-77-0119.

The variation of the temperature of the thermal electrons as a function of altitude has been reasonably well determined up to approximately 1500 km. Up to 800 km altitude, incoherent scatter radar stations have measured the temperature of the ionospheric electrons and up to 1500 km there have been numerous satellite reports on the electron temperature. However, prior to S3-3, there has been a lack of data about the electron temperature profile above ~1500 km. Some investigators have extrapolated the known temperature profiles up to the equatorial plane at altitudes of ~4 earth radii and estimated temperatures of several ten's of thousand degrees for the thermal electrons. From the Langmuir probe on S3-3, it was possible to measure the actual temperature of the thermal electrons in the plasmasphere up to 8000 km. Outside the plasmasphere, the electron density drops too rapidly for the Langmuir probe to make measurements at apogee, but measurements were made up to the limiting altitudes which provided some clue to the temperatures at very high altitudes.

The Langmuir probe on S3-3 is a gridded, spherical sensor on the end of a 1.2 meter boom as shown in Figure3-9. By measuring the current collected as a function of the voltage applied to the probe, the electron temperature and density and the vehicle potential with respect to the ambient plasma are measured. Basically the same instrument has been used on S3-2 and the DMSP satellites. The results of the measurements are accurate to 200^{o}K for temperature and a factor of 2 for density as long as the ambient density is in

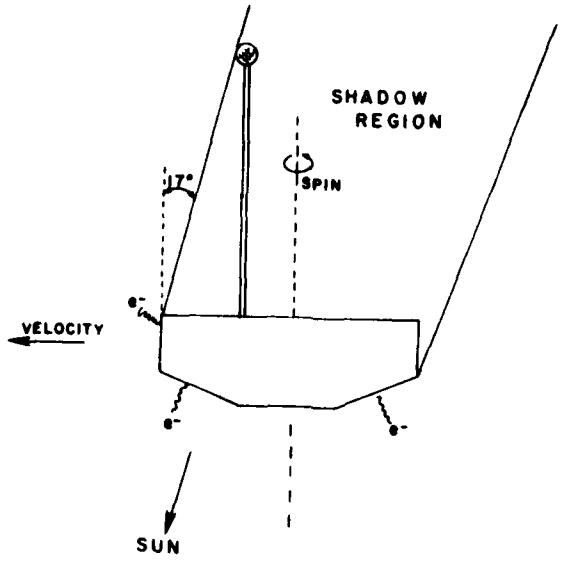

Figure 3-9: Configuration of the S3-3 satellite with the thermal electron probe deployed.

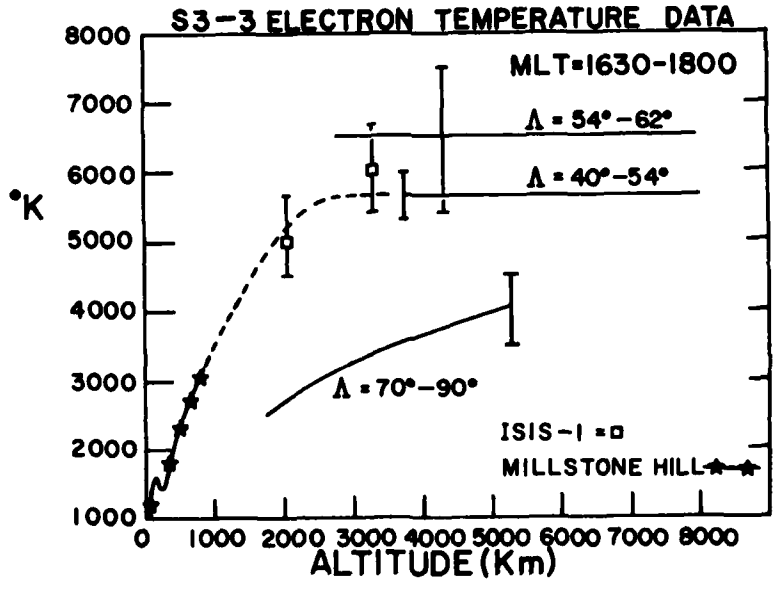

Figure 3-10: The profile of thermal electron temperatures as a function of altitude as determined by S3-3 in the late afternoon sector.

excess of 10^3 per cubic centimeter. Between 10^3 and 50 per cubic centimeter, the results can be degraded to the point of being useless due to photoelectrons from the vehicle and the grid wires of the sensor. Below 50 per cubic centimeter, no measurements can be made.

The results of the Langmuir probe are shown in Figure 3-10 and were presented in publications 8 and 31. At latitudes equatorward of the auroral zone, the electron temperature gradient along a magnetic field line at 1000 km decreases with increasing altitude until an altitude of approximately 3000 km. Above 3000 km, the gradient along a magnetic field line appears to become a constant of zero^{o}K per hour $\pm$ 0.1^{o}K per hour. Because the temperature gradient at 1000 km increases with increasing latitude, the temperature above 3000 km also varies as a function of latitude up to the auroral zone. In the auroral zone and mid-latitude trough regions between ~60^{o} and 72^{o} magnetic latitude, the Langmuir probe is unable to obtain good temperature measurements above 1000 km due to low densities and/or small scale length irregularities. In the polar cap, the number of good temperature measurements obtained is quite limited. Those that were obtained indicate that the electron temperature gradient does not significantly change with altitude in the polar cap region.

3. Analysis and Interpretation of the SSI/E Data from the DMSP Satellites.

The Defense Meteorological Satellite Program (DMSP) consists of a series of satellites whose primary purpose is to monitor the weather in the troposphere. The camera system on the satellite is sensitive enough to image the auroral displays on the night side of the earth. This imaging capability has been a valuable tool for studying the auroral ionosphere. In the last

few years, a series of secondary or special sensors have been added to the DMSP satellites to monitor the ionosphere in-situ. Starting with the Flight 2 and Flight 4 spacecrafts of the Block 5D series of DMSP satellites, the Air Force Geophysics Laboratory has provided sensors to measure the thermal ions and electrons. These sensors have been designed in part on this contract (See Section II on this report). The SSIE sensors are shown in Figure 3-11 on their boom in the deployed configuration on the Flight 2 satellite.

The DMSP F2 spacecraft was launched in June, 1977 into a circular orbit at 840 km. It was not injected into the required orbital plane with the consequence that the spacecraft has an unintentional drift in local time. At launch the spacecraft was near 07 and 19 hours local time; in 1979, it was near 10 and 22 hours local time. Also, as a result of the early orbit problems, SSIE data were not available until August, 1977.

The SSIE electronics and sensors have operated successfully from turn-on to the loss of the spacecraft in February, 1980. Thus with a few exceptions, there is a continuous data base covering two-and-a-half years. Typical examples of the kind of data available are shown in Figures 3-12a through 3-12d which show the total ion density at the spacecraft altitude versus time or latitude. The data have been plotted at the rate of one point per second although there are seven points available each second. Some of the most striking features from Figures 3-12a through 3-12d are:

a. A relatively smooth variation in density at mid-latitudes.

b. Highly variable density in both the northern and southern polar cap and auroral zones.

c. The mid-latitude ionospheric trough, most clearly seen in the evening sector.

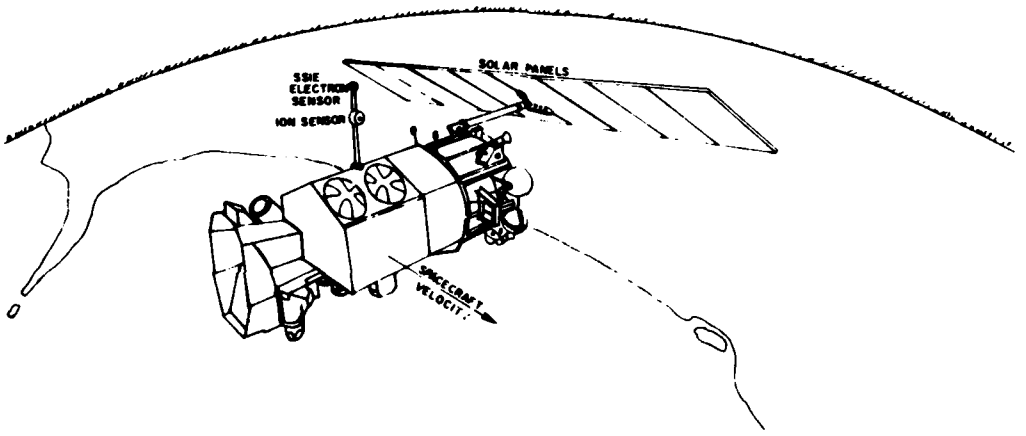

Figure 3-11: The Flight 2 DMSP satellite in orbit with the SSIE instrument

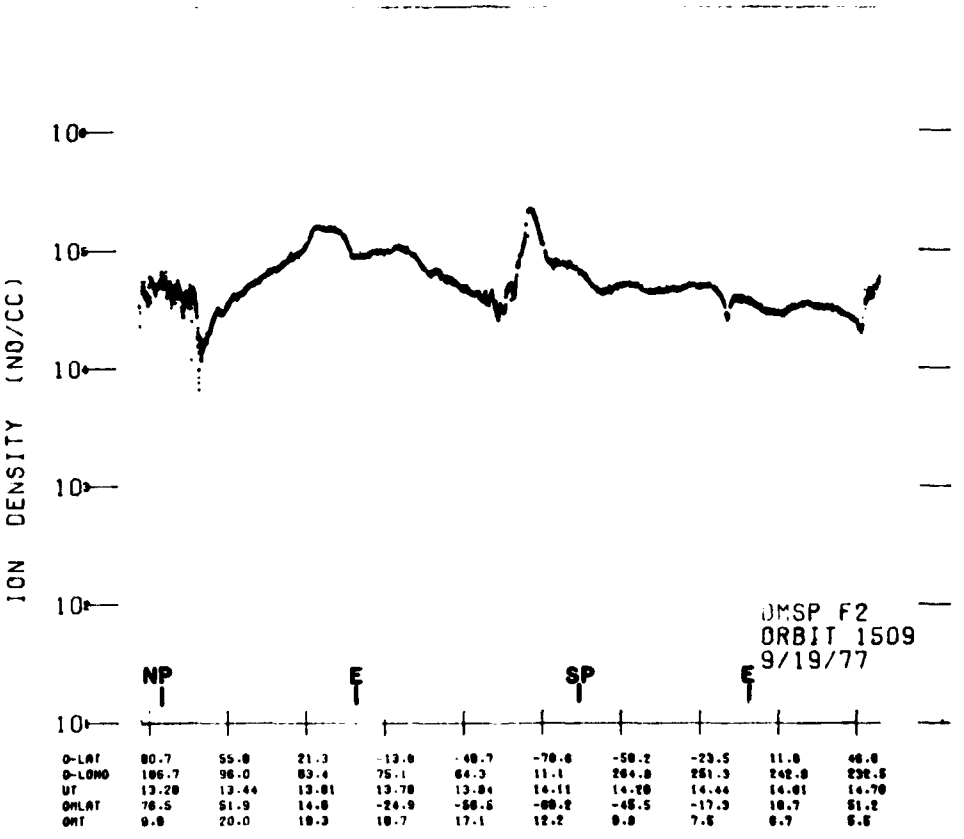

Figure 3-12a: The total ion density from the SSIE on the F2 DMSP satellite for orbit 1509.

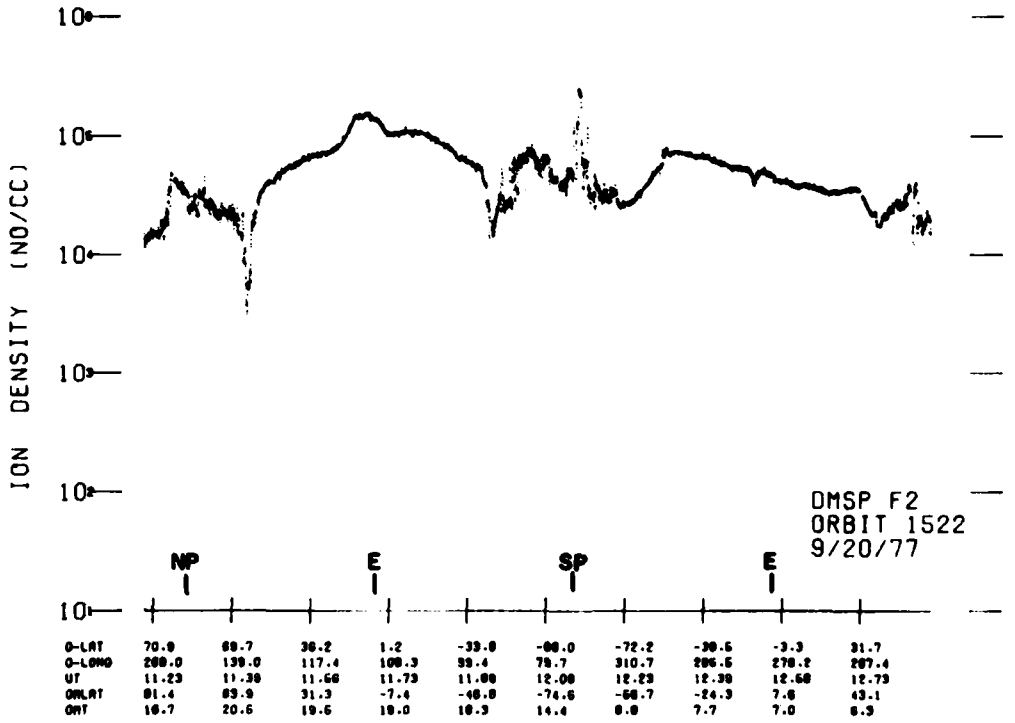

Figure 3-12b: The total ion density from the SSIE on the F2 DMSP satellite for orbit 1522.

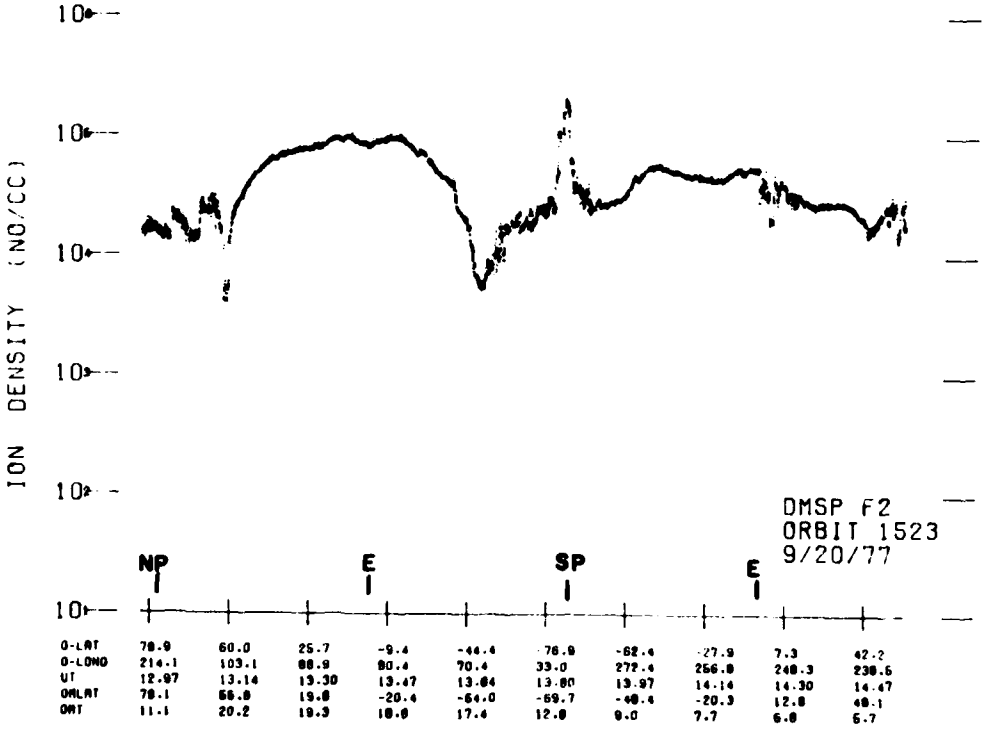

Figure 3-12c: The total ion density from the SSIE on the F2 DMSP satellite for orbit 1523.

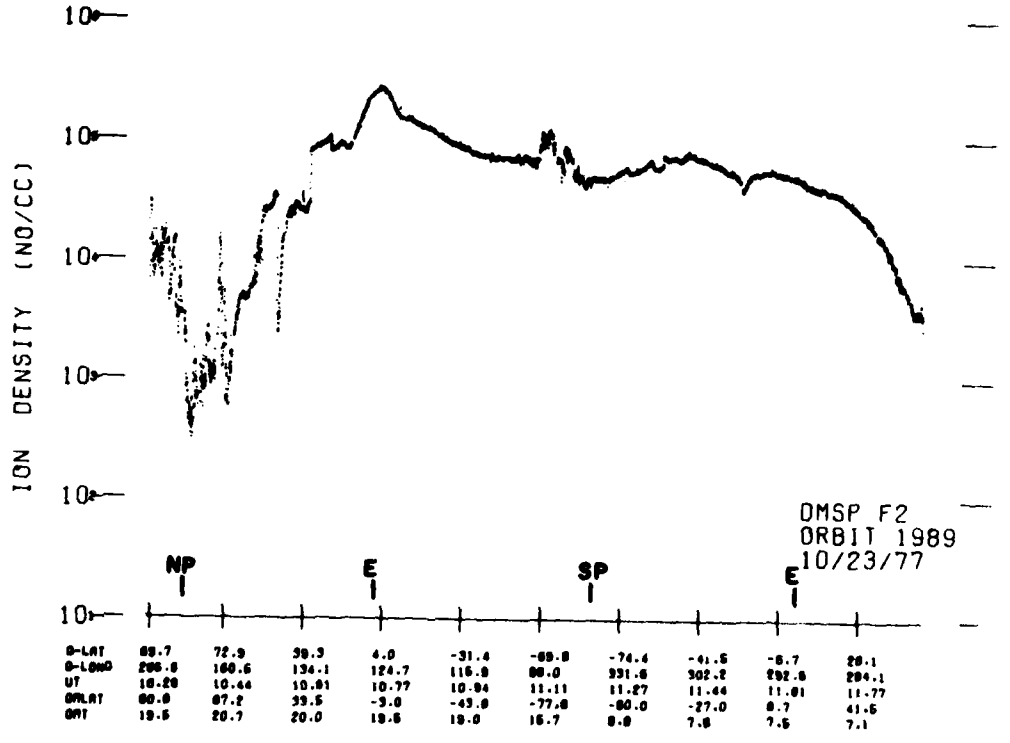

Figure 3-12d: The total ion density from the SSIE on the F2 DMSP satellite for orbit 1989.

d. A sharp, smooth density minimum near the sunrise equator on orbit 1522 and an irregular density minimum near the sunrise equator on orbit 1523 which is typical of "spread F" conditions.

Figure 3-13 is an example of the data as the spacecraft travels from darkness to sunlight. In darkness, the spacecraft potential is slightly negative due to the greater mobility of ambient electrons. Prior to launch, it was expected that spacecraft potential in sunlight would increase toward zero potential due to the emission of photoelectron from the vehicle. As seen in Figure 3-13, the current to the electron sensor in MODE 1 operation decreases to minimum sensitivity as the vehicle enters sunlight. When the vehicle first enters sunlight, the accelerating phase of the MODE 2 operation of the electron sensor does collect a few electrons, but after a few minutes in sunlight no electrons are collected at any time. This indicates that the vehicle potential was significantly less than -6V at the end of the period in Figure 3-13. Since the ion sensor was able to retard some of the ion flux at the end of the period in Figure 3-13, it would seem that the spacecraft potential was greater than -14V. However, the ion current versus retarding voltage curve does not fit a theoretical curve well enough to determine the actual spacecraft potential. This failure of the ion sensor data to yield meaningful information is due to two effects: First, the ion density and temperature calculated from the MODE 2 data apply to the plasma in the immediate vicinity of the ion sensor. These values are equivalent to the values of the "ambient" plasma only if the plasma entering the instrument is not disturbed by the presence of the spacecraft. In the presence of large accelerating potentials between the plasma and the instrument, a sheath is formed around the instrument and particles are drawn to the ion sensor and

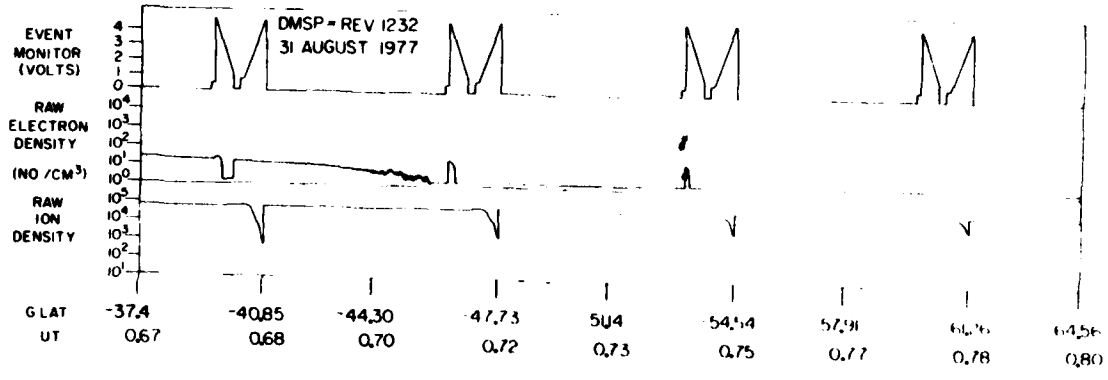

Figure 3-13: Plot of all data from the SSIE event monitor, electron sensor and ion sensor as the satellite crosses from night to daylight.

case from all directions in the sheath. For a planar probe with a small surface area in the forward direction compared to the DeBye length of the plasma, the sheath is approximately spherical in shape. Thus it is difficult to relate plasma parameters measured in the sheath to the ambient conditions.

Second, the assumption that no potential from the retarding screens leaks through the aperture screens to the ambient plasma is slightly in error at the largest potential difference between the retarding screens and the aperture screens.

The sunlight conditions shown in Figure 3-13 are typical of most of the data from the SSIE on the F2 satellite since the majority of data are taken in sunlight. An unknown, large negative (<-14 volts) potential invalidates all but the MODE 1 ion data. Even the MODE 1 ion data must be treated with caution since the ion flux to the sensor is enhanced by an unknown factor of the order of 100% by the effect of the large negative potential. Occasionally, a low flux of electrons are measured during sunlight conditions during both MODE 1 and MODE 2 operations. Generally, these fluxes have been found to be photoelectrons from the vehicle and sensor grids and/or super-thermal electrons which are typically found in the auroral zones and polar caps.

The large negative potential on the spacecraft encountered whenever the vehicle was in sunlight was found to be a result of two factors. First, there are a large number of interconnections between solar cells on the solar panels which are exposed to the ambient plasma. These interconnections can have up to +30 volts with respect to the spacecraft conducting frame which is the SSIE reference potential. Second, there is only a small conducting area ($\leq$3000 sq. inch) exposed to the ambient plasma on the entire F2 spacecraft.

The result is that a large negative charge is drawn from the ambient plasma at the interconnections when the solar cells are operating and there is insufficient exposed conducting area on spacecraft to reture the negative current to the plasma by drawing in ions or emitting photoelectrons.

Despite some uncertainty in the absolute density of ions near the spacecraft, the MODE 1 ion data from the SSIE on the F2-DMSP spacecraft provides an excellent representation of the distribution of ionization in the topside ionosphere as a function of latitude, longitude and season. Since the satellite is in a circular orbit, the data from on one orbit to another, one day to another, or one season to another can be compared without adjusting for varying altitudes such as is necessary from most spacecraft observations. The collection of data has been nearly continuous so that a complete survey of longitudes can be made from each day's data set. Figures 3-12b and 3-12c provide an example of the repeatability of the data on consecutive orbits. Figures 3-12a and 3-12d provide an example of the seasonal variations in the ionization morphology. Since the satellite orbit is nearly sun-synchronous, it is not possible to survey the ionization variations with local time. This limitation does allow an investigator to compare sets which are separated by many months because local time is not significantly different over such time spans.

The topside ionospheric morphology as described by the DMSP/F2 SSIE instrument has not been thoroughly investigated to date. One feature that has been investigated (see publications number 23 and 33) is the ionization depletion region near the morning side equator near equinox. This feature can be seen in Figures 3-12a, 3-12b and 3-12d. In Figure 3-12c, this feature is

obscured by spread F type ionization irregularities near the equator. The feature has been interpreted as region of low night-time ionization which has not been filled in due to the finite time for ionization to travel along field lines from the production region to the height of the satellite.

In response to the large negative spacecraft potential on the DMSP Block 5D spacecrafts while they are in sunlight, the SSIE was re-designed to be more compatible with the spacecraft. The re-design was constrained by the need to change the weight, power and size of the SSIE as little as possible in order to meet budget and scheduling requirements. For details of the engineering, see section II of this report. The most important change from the F2 instrument is the addition of a commandable set of bias potentials to float the SSIE sensor positively with respect to the DMSP spacecraft. Ideally, the bias voltages will be set so that the SSIE sensor will be within a few volts of the potential of the ambient plasma. Unfortunately this is not always possible for several reasons. First, there are only four possible bias voltage levels. This limitation allows the sensors to be as much as 6 volts from the plasma potential even with the best possible setting of the bias voltage. Second, operational requirements dictate a scheduling of the bias levels changes in advance where the spacecraft potential changes as a function of the potential across the solar panels which is not known in advance.

4. Summary

The scientific data analysis has been highly successful under this contract, but the potential value of the data sets used have been only partially exploited due to the large volume of high quality data available. The future

work that can be done with the S3-3 data seems to be limited to repeating the past work with a more complete data set. The future work that can be done with the S3-2 data and the DMSP/SSIE data is almost without limit.

IV.

PUBLICATIONS DONE IN WHOLE OR PART ON

CONTRACT F19628-77-C-0122

(1) SUB-AURORAL ELECTRIC FIELD OBSERVATIONS DURING A MAGNETIC STORM, M. SMIDDY, M.C. KELLEY, R.C. SAGALYN, P.J.L. WILDMAN, B.M. SHUMAN, W.J. BURKE, F.J. RICH, R. HAYES, AND S.T. LAI, EOS, 58 (6) 482, JUNE 1977.

(2) MODIFICATION OF THE IONOSPHERE - A PROPOSED METHOD FOR INJECTING WATER MOLECULES INTO THE IONOSPHERE, F.J. RICH, R.C. SAGALYN, AND P.J.L. WILDMAN, EOS, 58 (6) JUNE 1977.

(3) DIRECT OBSERVATIONS OF CONJUGATE PHOTOELECTRON HEATING IN THE WINTER NIGHTSIDE IONOSPHERE, W.J. BURKE AND R.C. SAGALYN, EOS, 58 (6) 453, JUNE 1977.

(4) ION MOTION MEASUREMENTS AT HIGH ALTITUDES FROM THE S3-3 SATELLITE, P.J.L. WILDMAN, R.C. SAGALYN, AND F.J. RICH, EOS, 58 (10), 991, OCTOBER 1977.

(5) LARGE AMPLITUDE IRREGULARITIES AT LOW LATITUDES IN THE TOPSIDE IONOSPHERE, W.J. BURKE, D.E. DONATELLI, R.C. SAGALYN, AND M.C. KELLEY, AFGL-TR-77-0263.

(6) TOPSIDE IONOSPHERIC TROUGH MORPHOLOGY AT MID- AND HIGH-LATITUDES, M. AHMED AND R.C. SAGALYN, PREPRINTS OF PROCEEDINGS, 1978 SYMPOSIUM ON THE EFFECT OF THE IONOSPHERE ON SPACE AND TERRESTRIAL SYSTEMS, JOINTLY SPONSORED BY NRL AND ONR, WASHINGTON, D.C., JANUARY 24-26, 1978.

(7) INTENSE POLEWARD - DIRECTED ELECTRIC FIELDS NEAR THE IONOSPHERIC PRO - JECTION OF THE PLASMA-PAUSE, M. SMIDDY, M.C. KELLEY, W.J. BURKE, F. RICH, R. SAGALYN, B. SHUMAN, R. HAYS AND S. LAI, GEOPHYS. RES. LTR, 4, (11), 543-546, 1977.

(8) ELECTRON TEMPERATURE PROFILES MEASURED UP TO 8000 KM BY S3-3, F. RICH, W.J. BURKE, P.J.L. WILDMAN AND R.C. SAGALYN, EOS, 59, (4) 338, APRIL 1978.

(9) OBSERVATIONS FROM THE INJUN 5 SATELLITE CONCERNING THE RELATIVE POSITIONS OF THE QUIET TIME RING CURRENT AND THE TOPSIDE ELECTRON TEMPERATURE MAXIMUM IN THE TROUGH, W.J. BURKE, H.J. BRAUN, J.W. MUNCH, AND R.C. SAGAGLYN, EOS, 59, (4), 337, APRIL 1978.

(10) ELECTRIC FIELDS AT HIGH LATITUDES NEAR THE DAWN DUSK MERIDIAN, M. SMIDDY, W.J. BURKE, M.C. KELLEY, AND S.T. LAI, EOS, 59 (4), 360-361, APRIL 1978.

(11) CORRELATED OBSERVATIONS OF THE VISIBLE AURORAE IN THE EVENING SECTOR MADE WITH THE DMSP AND S3-2 SATELLITES, D.A. HARDY, W.J. BURKE, B. SHUMAN, R. VANCOUR, AND M. SMIDDY, EOS, 59 (4), 357, APRIL 1978.

(12) ALTITUDE VARIATIONS OF THE TOPSIDE IONOSPHERIC TROUGH CHARACTERISTICS, M. AHMED, R.C. SAGALYN AND P.J.L. WILDMAN, EOS, 59, (4), 349, APRIL 1978.

(13) THE BEHAVIOR OF GRIDDED SPHERICAL AND PLANAR ELECTRON PROBES IN A NON-MAXWELLIAN PLASMA, W.J. BURKE AND M. SMIDDY, AFGL-TR-78-0064.

(14) TOPSIDE IONOSPHERIC TROUGH MORPHOLOGY - OCCURRENCE FREQUENCY, DIURNAL SEASONAL AND ALTITUDE VARIATIONS, M. AHMED, R.C. SAGALYN, AND P.J.L. WILDMAN, J. GEOPHYS. RES., 84 (A2), 489-498, 1979.

(15) INJUN 5 LOW ENERGY PLASMA OBSERVATIONS DURING A MAJOR MAGNETIC STORM, L.D.V. RAO, W.J. BURKE AND M. KANAL, J. GEOPHYS. RES., 83, (A7), 3217-3225, 1978.

(16) ELECTRIC FIELDS AT HIGH LATITUDES IN THE TOPSIDE IONOSPHERE NEAR THE DAWN-DUSK MERIDIAN, W.J. BURKE, R.C. SAGALYN, M. SMIDDY, M.C. KELLEY AND S.T. LAI, SPACE RESEARCH, 19, 1978;

(17) POLAR CAP ELECTRIC FIELD STRUCTURES WITH A NORTHWARD INTERPLANETARY MAGNETIC FIELD, W.J. BURKE, M.C. KELLEY, R.C. SAGALYN, M. SMIDDY AND S.T. LAI, GEOPHYS. RES. LETTERS, 6 (1), 21-24, 1979;

(18) THE TOPSIDE IONOSPHERE PLASMA MONITOR (SSIE) FOR THE BLOCK 5D FLIGHT 2 DMSP SATELLITE, M. SMIDDY, R.C. SAGALYN, W.P. SULLIVAN, P.J.L. WILDMAN, P. ANDERSON AND F. RICH, AFGL-TR-78-0071;

(19) INJUN 5 OBSERVATIONS OF LOW-ENERGY PLASMA IN THE HIGH-LATITUDE TOPSIDE IONOSPHERE, W.J. BURKE, D.E. DONATELLI, AND R.C. SAGALYN, J. GEOPHYS. RES., 83 (A5), 2047-2056, 1978;

(20) TOPSIDE IONOSPHERIC TROUGH MORPHOLOGY AT MID AND HIGH LATITUDES, M. AHMED AND R.C. SAGALYN, AFGL-TR-78-0080.

(21) SUBSTORM SIMULATION RESULTS: II. SUBAURORAL ELECTRIC FIELDS AND EVOLUTION OF THE PLASMAPAUSE, R.W. SPIRO, M. HAREL, R.A. WOLF, P.H. REIFF, AND F.J. RICH, EOS, 60 (18), 327, May 1979;

(22) OBSERVATIONS OF FIELD-ALIGNED CURRENTS IN ASSOCIATION WITH STRONG CONVECTION ELECTRIC FIELDS IN THE TROUGH, M. SMIDDY, F.J. RICH, W.J. BURKE, D.A. HARDY, AND R.A. WOLF, EOS, 60, (18), 327, May 1979.

(23) OBSERVATIONS OF FLUX TUBE REFILLING AFTER SUNRISE IN THE EQUATORIAL TOPSIDE IONOSPHERE, R.C. SAGALYN, R.G. RASTOGI, M. AHMED, F.J. RICH, D.E. DONATELLI, AND P.J.L. WILDMAN, EOS, 60 (18), 335, May 1979;

(24) THE LONGITUDINAL DISTRIBUTION OF TOPSIDE PLASMA BUBBLES, D.E. DONATELLI, W.J. BURKE, AND R.C. SAGALYN, EOS, 60 (18), 335, MAY 1979.

(25) THE CONTRIBUTIONS OF SATELLITE SIZE, SATELLITE POTENTIAL AND PLASMA PARAMETERS IN DETERMINING ION DISTRIBUTION AROUND THE S3-2 SATELLITE -- AN EXPERIMENTAL ASSESSMENT, U. SAMIR, P.J.L. WILDMAN, R.C. SAGALYN AND F.J. RICH, EOS, 60 (18), 335, MAY 1979;

(26) ELECTRIC AND MAGNETIC FIELD STRUCTURE AT HIGH LATITUDES WITH A NORTHWARD IMF, M.S. GUSSENHOVEN, W.J. BURKE, D.A. HARDY, AND F.J. RICH, EOS, 60 (18), 349, MAY 1979;

(27) ELECTRODYNAMIC STRUCTURES IN THE LATE EVENING SECTOR OF THE AURORAL ZONE, W.J. BURKE, D.A. HARDY, F.J. RICH, AND M.C. KELLEY, EOS, 60 (18), 351, MAY 1979;

(28) OBSERVED ELECTRIC AND MAGNETIC FIELD STRUCTURE OVER THE HARANG DISCONTINUITY, F.J. RICH, W.J. BURKE AND D.A. HARDY, EOS, 60 (18), 355, MAY 1979;

(29) AURORAL DYNAMICS DURING A SUBSTORM NEAR THE DAWN-DUSK MERIDIAN, D.A. HARDY, F.J. RICH AND W.J. BURKE, EOS, 60 (18), 358, May 1979;

(30) OBSERVED HEATING EFFECTS OF CONJUGATE PHOTOELECTRONS, W.J. BURKE, R.C. SAGALYN, AND M. KANAL, PLANET. SPACE SCI., 27, 583, 1979;

(31) ELECTRON TEMPERATURE PROFILES MEASURED UP TO 8000 km BY S3-3 IN THE LATE AFTERNOON SECTOR, F.J. RICH, R.C. SAGALYN, AND P.J.L. WILDMAN, J. GEOPHYS. RES., 84(A4), 1328, APRIL 1979.

(32) LOW DENSITY REGIONS OBSERVED AT HIGH ALTITUDES AND THEIR CONNECTION WITH EQUATORIAL SPREAD F, W.J. BURKE, D.E. DONATELLI, R.C. SAGALYN, AND M.C. KELLEY, PLANET. SPACE SCI., 27, 593, 1979,

(33) POSTSUNRISE REFILLING OF THE LOW-LATITUDE, TOPSIDE IONOSPHERE, W.J. BURKE, R.C. SAGALYN, R.G. RASTOGI, M. AHMED, F.J. RICH, D.E. DONATELLI, AND P.J.L. WILDMAN, J. GEOPHYS. RES., 84 (A8), 4201, AUGUST 1, 1979. (CORRECTION, J. GEOPHYS. RES., 84, A12, 7386, 1979)

(34) OBSERVATIONS CONCERNING THE RELATIONSHIP BETWEEN THE QUIET-TIME RING CURRENT AND ELECTRON TEMPERATURES AT TROUGH LATITUDES, W.J. BURKE, H.J. BRAUN, J.W. MUNCH, AND R.C. SAGALYN, PLANET. SPACE SCI., 27, 1175, 1979.

(35) PLASMA BUBBLES NEAR THE DAWN TERMINATOR IN THE TOPSIDE IONOSPHERE, W.J. BURKE, PLANET SPACE SCI., 27, 1187, 1979.

(36) ELECTRODYNAMIC STRUCTURE OF THE LATE EVENING SECTOR OF THE AURORAL ZONE, W.J. BURKE, D.A. HARDY, F.J. RICH, M.C.KELLEY, M. SMIDDY, B. SHUMAN, R.C. SAGALYN, R.P. VANCOUR, P.J.L. WILDMAN AND S.T. LAI, J. GEOPHYS. RES., 85, (A3), 1179, 1980.

(37) OBSERVATIONS OF FIELD-ALIGNED CURRENTS IN ASSOCIATION WITH STRONG CONVECTION ELECTRIC FIELDS AT SUBAURORAL LATITUDES, F.J. RICH, W.J. BURKE, M.C. KELLEY, M. SMIDDY, J. GEOPHYS. RES., 85, (A5), 2335, 1980.

(38) HEIGHT VARIATIONS OF FIELD ALIGNED CURRENTS AND ELECTROSTATIC SHOCKS OBTAINED FORM SIMULTANEOUS OBSERVATIONS, F.J. RICH, C.A. CATTELL, W.J. BURKE, M. SMIDDY, EOS, 61, 17, 332, 1980.

(39) FIELD ALIGNED CURRENTS OBSERVED IN THE REGION OF THE DAYSIDE CUSP, M.A. DOYLE, F.J. RICH, W.J.BURKE, M. SMIDDY, EOS, 61, 17, 333, 1980.

(40) OBSERVATIONS OF EQUINOCTAL DENSITY ENHANCEMENTS IN THE EQUATORIAL TOPSIDE IONOSPHERE NEAR THE SUNSET TERMINATOR, E.R. YOUNG, F.J. RICH, M. SMIDDY, R.C. SAGALYN, EOS, 61, 17, 320, 1980.